



HAL
open science

Origin of CO₂, CH₄, and N₂O trapped in ice wedges in central Yakutia and their relationship

Ji-Woong Yang, Jinho Ahn, Go Iwahana, Nayeon Ko, Jihoon Kim, Kyungmin Kim, Alexander Fedorov, Sangyoung Han

► **To cite this version:**

Ji-Woong Yang, Jinho Ahn, Go Iwahana, Nayeon Ko, Jihoon Kim, et al.. Origin of CO₂, CH₄, and N₂O trapped in ice wedges in central Yakutia and their relationship. *Permafrost and Periglacial Processes*, 2023, 34, pp.122-141. 10.1002/ppp.2176 . hal-04122369

HAL Id: hal-04122369

<https://hal.science/hal-04122369>

Submitted on 22 Jun 2023







HAL is a multi-disciplinary open access archive for the deposit and dissemination of scientific research documents, whether they are published or not. The documents may come from teaching and research institutions in France or abroad, or from public or private research centers.

L'archive ouverte pluridisciplinaire **HAL**, est destinée au dépôt et à la diffusion de documents scientifiques de niveau recherche, publiés ou non, émanant des établissements d'enseignement et de recherche français ou étrangers, des laboratoires publics ou privés.

RESEARCH ARTICLE

WILEY

Origin of CO₂, CH₄, and N₂O trapped in ice wedges in central Yakutia and their relationship

Ji-Woong Yang^{1,2}  | Jinho Ahn^{1,3}  | Go Iwahana⁴  | Nayeon Ko¹ |
 Ji-Hoon Kim⁵  | Kyungmin Kim^{1,6}  | Alexander Fedorov⁷  | Sangyoung Han¹

¹School of Earth and Environmental Science, Seoul National University, Seoul, South Korea

²Laboratoire des Sciences du Climat et de l'Environnement, Institut Pierre-Simon Laplace, UMR CEA-CNRS-UVSQ 8212, Gif-sur-Yvette, France

³Center for Cryospheric Sciences, Seoul National University, Siheung, South Korea

⁴International Arctic Research Center, University of Alaska Fairbanks, Fairbanks, AK, USA

⁵Marine and Petroleum Resources Research Division, Korea Institute of Geoscience and Mineral Resources, Daejeon, South Korea

⁶Geophysical Institute, Department of Geosciences, University of Alaska Fairbanks, Fairbanks, AK, USA

⁷Melnikov Permafrost Institute, Russian Academy of Science, Yakutsk, Russia

Correspondence

Jinho Ahn, School of Earth and Environmental Science, Seoul National University, Seoul, South Korea.

Email: jinhoahn@snu.ac.kr

Present address

Kyungmin Kim, Geophysical Institute, Department of Geosciences, University of Alaska Fairbanks, Fairbanks, AK, USA.

Funding information

This study is supported by National Research Foundation of Korea (2020M1A5A1110607; 2018R1A5A1024958) and Korea Ministry of Oceans and Fisheries (1525011795).

Abstract

Permafrost thawing as a result of global warming is expected to foster the biological remineralization of intact organic carbon and nitrogen and release greenhouse gas (GHG) into the atmosphere, which will have positive feedback for future global warming. However, GHG budgets and their controls in permafrost ground ice are not yet fully understood. This study aims to better understand the control mechanisms of GHG in ground ice by using new gas and chemistry data. In this study, we present new data on carbon dioxide (CO₂), methane (CH₄), and nitrous oxide (N₂O) mixing ratios in three different ice wedges, Churapcha, Syrdakh, and Cyuie, located in central Yakutia, Siberia. The GHG mixing ratios in the studied ice wedges range from 0.0% to 13.8% CO₂, 1.3–91.2 ppm CH₄, and 0% and 0–1414 ppm N₂O. In particular, all three ice wedges demonstrate that ice-wedge samples enriched in CH₄ were depleted in N₂O mixing ratios and vice versa. N₂–O₂–Ar compositions indicate that the studied ice wedges were most likely formed by dry snow or hoarfrost, not by freezing of snow meltwater, and the O₂-consuming biological metabolism was active. Most of the observed GHG mixing ratios cannot be explained without microbial metabolism. The inhibitory impact of denitrification products of nitrate (including N₂O) could be an important control of the ice-wedge CH₄ mixing ratio.

KEYWORDS

carbon dioxide, central Yakutia, ice wedges, methane, nitrous oxide, permafrost

1 | INTRODUCTION

Permafrost is a large terrestrial reservoir of organic carbon (C) and nitrogen (N), which are temporarily intact from active global C- and N-cycles.^{1,2} Accumulating evidence shows that the remobilization of organic C and N on permafrost thawing could release significant amounts of greenhouse gases (GHG) into the atmosphere and provide positive feedback for the global warming.^{3,4} Particular focus has been

devoted to Yedoma, the organic and ice-rich Pleistocene permafrost deposits across Beringia.⁵ At present, Yedoma covers ~1,387,000 km² or ~6% of the permafrost region in the Northern Hemisphere (~23 × 10⁶ km²).⁶ Yedoma is particularly abundant in eastern Siberia and Alaska,⁷ but also in central Yakutia.^{8–12} Despite its relatively small proportions, the organic-rich Yedoma preserves ~327–466 Gt of organic carbon,^{6,13} accounting for over ~25% of organic carbon stored in northern high-latitude permafrost

(~1,140–1,476 Gt).¹ Furthermore, its higher ice content (~80 vol %),^{6,14} compared to other permafrost soils, causes Yedoma to be highly vulnerable to abrupt climate warming.^{15,16} Given that the high-latitude regions are more sensitive to global warming than the rest of the world,¹⁷ how Yedoma deposits respond to global warming is the key to accurately projecting future climate change. However, to date, despite this high ice content, most studies dealing with C and N in permafrost have focused on sediments or soils, and the mechanisms for GHG production and consumption in ice wedges, one of the most common types of ground ice, have yet to be elucidated. The ice-wedge volume has been estimated as ~48 vol%, larger than that of segregated ice (~34 vol%) in Yedoma.⁶

Ice wedges are formed and grow by repeated cycles of frost cracking of frozen ground by thermal contraction in winter and snow meltwater infiltration in spring that quickly refreezes due to subzero temperature and creates vertical ice veins.¹⁸ As the frost cracking tends to occur near the center of the ice wedges, the central part of an ice wedge has generally been created more recently (i.e., younger age) than the outer margins; however, the stratigraphy is often more complex.¹⁹ The frost cracks can also be infilled by snow densification or hoarfrost accretion depending on regional climate.^{20,21} The infilling material may include sediments, minerals, and organic material that enables *in situ* microbial activities and radiocarbon dating.^{19,22} Moreover, the interstitial air within snow and hoarfrost or dissolved gas in snow meltwater is incorporated into the ice veins, allowing diverse studies on gas properties.^{20,21,23,24}

Studies have directly measured the mixing ratios of more than two GHGs from ground ice.^{20,23,25} Brouchkov and Fukuda²⁵ reported the CO₂ and CH₄ mixing ratios of ice wedges from three different sites in central Yakutia and found that the CO₂ and CH₄ mixing ratios were higher than atmospheric levels, implying *in situ* respiration (for CO₂) and the occurrence of anaerobic conditions (for CH₄) in ground ice. Furthermore, the CO₂ and CH₄ mixing ratios exhibit a weak negative relationship (i.e., high CO₂ mixing ratios with low CH₄, and vice versa), from which they speculated that the *in situ* CH₄ oxidation process occurred. Boereboom et al.²⁰ carried out a multiproxy study, including water-stable isotopes, crystallography, and gas properties, on two ice wedges in northern Siberia. Similar to Brouchkov and Fukuda,²⁵ they also observed higher CO₂ and CH₄ mixing ratios than in the atmosphere and regarded the CO₂ and CH₄ mixing ratios as indicators of microbial respiration and methanogenesis, respectively. Our previous study²³ reported for the first time the mixing ratios of CO₂, CH₄, and N₂O from two adjacent ice-wedge outcrops in Cyuie, central Yakutia. The strong point of Kim et al.'s²³ data was the simultaneous measurements of the three GHGs in one ice sample, which allows a more precise comparison between GHGs than each gas species measured from a different (mostly adjacent) ice piece. This is because the simultaneous analysis rules out any potential bias due to centimeter-scale inhomogeneity of GHG compositions. Kim et al.²³ also reported for the first time a clear negative relationship between CH₄ and N₂O mixing ratios, suggesting that methanogenesis may be inhibited by N₂O. However, this negative relationship between CH₄

and N₂O has only been observed in this study site and will require further analysis to verify the findings more broadly.

The aims of the present study were: (i) to test whether the negative CH₄–N₂O relationship is a common feature of permafrost ice wedges at a regional scale, and (ii) to better understand the mechanisms that control the CH₄ and N₂O mixing ratios. To achieve these objectives, we measured the CO₂, CH₄, and N₂O compositions in multiple ice wedges located in central Yakutia, using recently published dry gas extraction and correction methods dedicated to ground ice.²⁶ Ice-wedge samples were used because the ice wedge is ubiquitous and is one of the most common forms of massive ground ice in Siberia and Alaska, comprising ~31.4 to 63.2 vol% of Yedoma deposits.²⁷ In addition, as complementary data, we analyzed the major ion concentrations and pH of the meltwater of adjacent ice samples. Because of the inhomogeneity of the chemical properties of ground ice, the water chemistry results were not compared to the adjacent GHG records but instead averaged to understand the geochemical characteristics of each study site.

Compared to our previous study,²³ here we not only present additional GHG data from the identical ice wedge that was studied by Kim et al.²³ but also provide new results from two different sites to confirm our previous findings and to test the generality of the features observed between GHGs. Furthermore, together with new geochemical data of wedge ice, we present further discussion about the potential mechanism of *in situ* formation of GHGs.

2 | MATERIALS AND METHODS

2.1 | Study area

Ice-wedge samples were collected from three different sites in central Yakutia: Churapcha, Cyuie, and Syrdakh (Figure 1). The study sites are located within ~150 km of each other around the Lena-Amga interfluvium. Central Yakutia is located in a continuous permafrost zone, where the permafrost thickness reaches 400 to 500 m²⁸ and is largely covered by Yedoma deposits. The high ice content of the Yedoma deposit makes this region particularly vulnerable to *alás* (drained thermokarst basin) created by thermokarst lake development, land depression, lake drainage, and refreezing.²⁹ This region is strongly affected by a dry continental climate with a mean annual air temperature of -9.8 ± 1.8 (1 σ)°C (1910–2014 mean³⁰). The permafrost temperature (subsoil temperature) and active-layer thickness of the Lena-Amga interfluvium region range from -3°C to -2°C and from 1 to 2 m, respectively (1960–1987 mean³¹).

Site Churapcha is located 180 km east of Yakutsk in a periglacial plain with an ice complex found ~2 m below the surface (61.97°N, 132.61°E). In October 2016, a total of 34 ice-wedge cores of 8 cm diameter were drilled perpendicularly ~40 cm from the outcrop surface and around 30 to 50 cm below the top of the ice complex. The first 10 cm from the wall surface was removed before analysis (Figure 2a). This area has typical *alás* landforms on the right bank of the Tatta River. The sampling site was located at a bluff of the

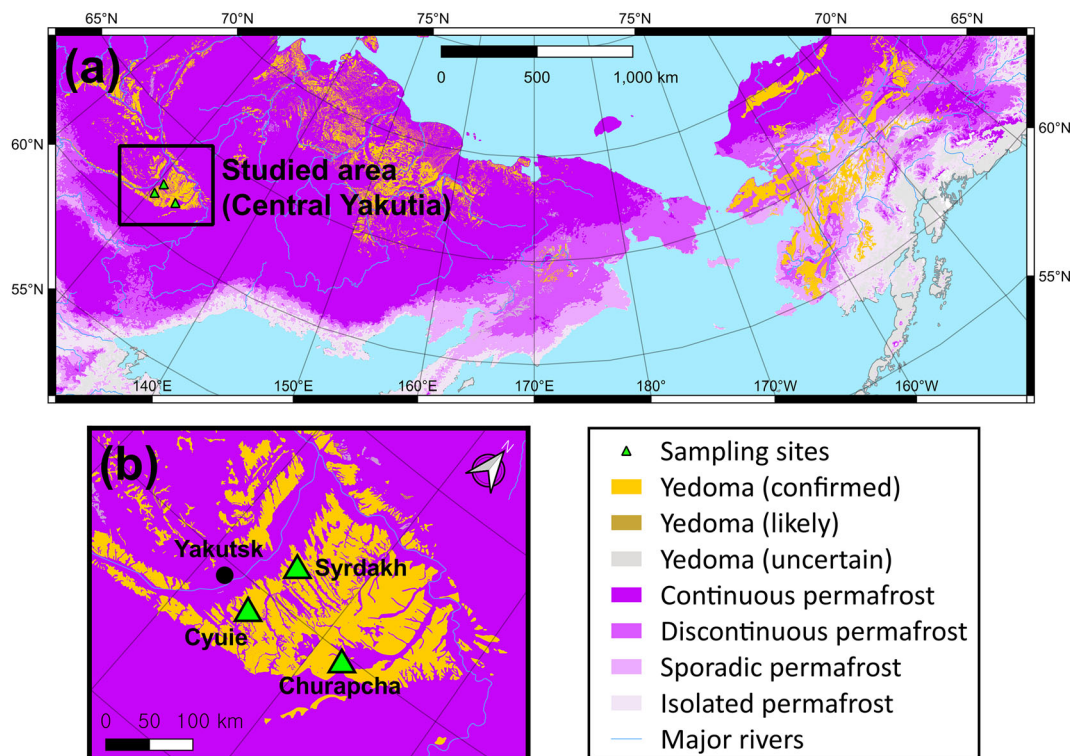


FIGURE 1 (a) Map showing the permafrost,³² Yedoma³³ distribution around the circum-Arctic region, and the area studied in this article (central Yakutia) in black; (b) the enlarged map of the studied area showing the sampling sites of Churapcha, Cyuie, and Syrdakh [Colour figure can be viewed at wileyonlinelibrary.com]

thermocarst Lake Bietege, where the head wall actively collapses owing to lateral thermal erosion of the ice complex. Site Syrdakh is located in the Alas Kychyma 100 km northeast of Yakutsk on the Tyunglunskiy³⁴ terrace of the Lena River (62.33°N, 130.58°E) (Figure 2b). The Alas Kychyma is located in the middle of the valley of the rivulet Syrdakh. Eight ice-wedge blocks were sampled ~1 m below the surface using a chain saw. Our sampling location was on a bluff of the thermocarst lake Kychyma, where lateral thermal erosion was active. Site Cyuie is located near Cyuie village, ~30 km away from Yakutsk (61.73°N, 130.42°E) (Figure 2c). In July 2015, nine blocks of wedge ice were cut with a chainsaw from two exposed ice wedges found ~1 m below the surface.²³ The CYB samples were cut ~1 m below the top of the ice wedge, and the CYC samples were ~50 cm below the top.

2.2 | Greenhouse gas mixing ratios

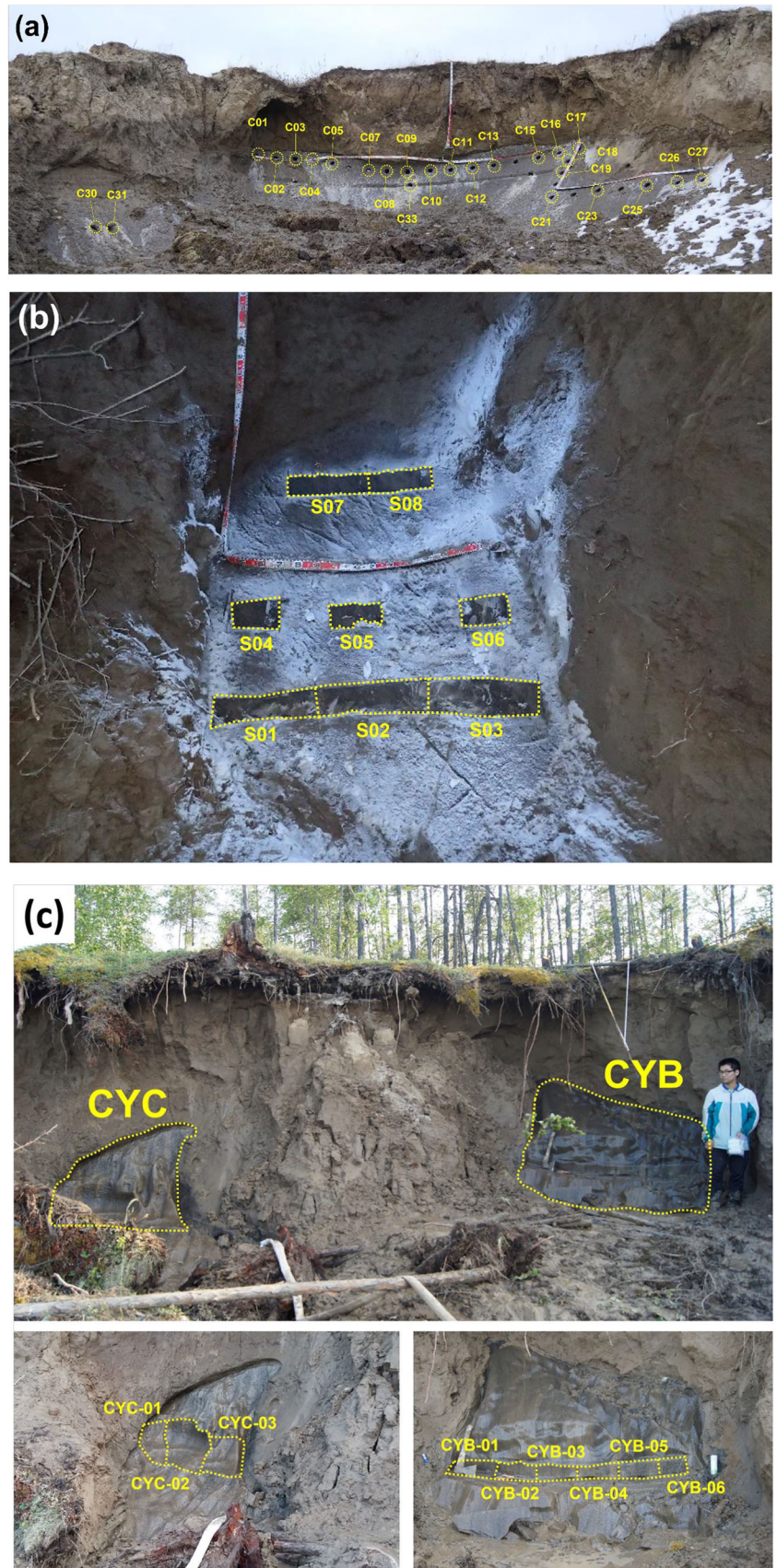
The enclosed air in the wedge ice was liberated by a dry extraction system at Seoul National University (SNU, Seoul, South Korea), following the analytical procedures and corrections described by Yang et al.²⁶ Details of the SNU dry extraction system are described in Shin.³⁵ We employed dry extraction rather than wet extraction (melting–refreezing) because of the high solubility of CO₂ in water and carbonate-forming reactions that preclude the precise

determination of the CO₂ mixing ratio. For CH₄ and N₂O, the dry and wet extraction techniques yielded no significant difference.²⁶ In addition, Yang et al.²⁶ found no evidence of CH₄ contamination by metal friction, as suggested by Higaki et al.³⁶

We followed dry extraction with the hitting method, as described by Yang et al.,²⁶ and repeated it five times, with some modifications. Briefly, one or two pieces of ice-wedge samples (~10 g) were crushed in a vacuum chamber using a needle crusher. The temperature of the vacuum chamber was maintained at –37°C by circulating chilled ethanol. Owing to the low air content, pure nitrogen (N₂) gas (99.9999% purity) was injected into the chamber to dilute the sample air. The pressure of the gas mixture within the chamber was monitored using a Baratron manometer before and after dilution. The water vapor in the gas mixture was removed by passing through a water trap maintained under –80°C using an ethanol and liquid N₂ mixture. After drying, the gas mixture was cryogenically trapped within stainless steel tubes immersed in a helium closed-cycled refrigerator (He-CCR). The internal temperature of the He-CCR was maintained under –262°C through gas extraction.

The mixing ratios of CO₂, CH₄, and N₂O in the Siberian ice wedges were measured simultaneously from a single ice sample using two GC systems. The sample tubes were first connected to a GC system (Agilent 7890A, Agilent Technologies Inc., Santa Clara, CA, USA) equipped with a methanizer and a flame ionization detector (GC-FID) for CO₂ analysis. Then, the remaining gas in the sample tube

FIGURE 2 (a) Photograph of the Churapcha ice-wedge outcrop. The core sampling locations are denoted in yellow-dotted circles. Picture modified from Yang et al.²⁶ (b) Photograph of the Syrdakh ice-wedge outcrop. The ice sampling locations are denoted in yellow-dotted lines. (c) Top: photographs of the Cyuie sampling site showing two ice-wedge outcrops (CYB and CYC). Bottom: detailed pictures of each outcrop and sampling locations. Figure adapted from Yang et al.²⁶ [Colour figure can be viewed at wileyonlinelibrary.com]



was expanded into the second GC system equipped with an electron capture detector (ECD) and FID (GC-ECD-FID, Agilent 7890B) for CH₄ and N₂O measurements. Detailed settings of the GC-FID system can be found in Ahn et al.,³⁷ and Shin,³⁵ and those of the GC-ECD-FID system are described in Ryu et al.³⁸

In a previous study, we found that the CH₄ and N₂O mixing ratios resulting from the SNU dry extraction system are affected by systematic blanks during needle crushing.²⁶ The blanks of CH₄ and N₂O mixing ratios were inversely dependent on the quantity of gas (i.e., gas pressure) trapped in the sample tubes. The CH₄ and N₂O results in the present study were corrected using the formulation provided by Yang et al.²⁶ The average soil crushing effects for CH₄ and N₂O were 1.1 ± 0.3 ppm and 10.9 ± 4.1 ppb, respectively.

2.3 | Molar ratios of N₂, O₂, and Ar

The molar ratios of N₂, O₂, and Ar were measured in selected samples to discern the formation mechanism of the ice wedge. Approximately 100–150 g of ice was prepared at each ice-wedge site and cut into 8 to 15 subsamples to fit into the crushing chamber of the dry extraction system. The ice subsamples of each ice wedge were crushed in a row, and the enclosed gases were trapped in a single sample tube following the procedures described earlier. In this case, the sample gas was not diluted. The molar ratios of Ar to N₂ (δ [Ar/N₂]) and O₂ to N₂ (δ [O₂/N₂]) were measured using an isotope ratio mass spectrometer (Finnigan Delta V, Thermo Scientific, Waltham, MA, USA) at the Scripps Institution of Oceanography (SIO, San Diego, CA, USA) with regard to modern air. Detailed analytical methods are described in Sowers et al.³⁹ and Petrenko et al.³⁹

2.4 | Major ion chemistry

As it is difficult to collect the leftover ice after dry extraction, we prepared ~50 g of wedge ice samples adjacent to the GHG samples for ice chemistry analysis. The GHG and chemistry samples were normally less than 3 cm apart. The surfaces of the ice samples were rinsed with distilled deionized water, melted in glass beakers that were cleaned with acid (1 N hydrochloric acid; HCl), and rinsed with distilled deionized water more than three times. Ice melting was performed in a fume hood at room temperature. The meltwater and soil were separated by centrifugation at 3,000 rpm for 10 min. The meltwater samples were filtered with 0.45 μm polypropylene syringe filters and collected in high-density polyethylene (HDPE) bottles (Nalgene, Rochester, NY, USA). The pincers and HDPE bottles were precleaned using the same procedure as the beakers. The anion concentrations (F⁻, Cl⁻, NO₃⁻, Br⁻, SO₄²⁻, and PO₄³⁻) in the Churapcha and Syrdakh samples were analyzed using an ion chromatograph at the Korean Institute of Geoscience and Mineral Resources (KIGAM, Daejeon, South Korea), and cations (Ca²⁺, K⁺, Mg²⁺, and Na⁺) were measured at the Korea Basic Science Institute (KBSI). The NH₄⁺ and additional

NO₃⁻ analyses for the Churapcha, Cyuie, and Syrdakh samples were performed using an ion chromatograph (ICS-5000, Dionex Corporation, Sunnyvale, CA, USA) at the National Instrumentation Center for Environmental Management (NICEM) at SNU.

2.5 | Radiocarbon age dating

The ages of the studied ice wedges were dated by radiocarbon (¹⁴C) decay of visible plant remaining enclosed in the wedge ice and the gaseous phase (¹⁴C-CO₂). The plant residues enclosed in selected ice-wedge ice samples were collected in the oven-dried soils by sieving and picked under a stereoscopic microscope. The collected plant residues were pretreated and radiocarbon dated at Beta Analytic Inc. For ¹⁴C-CO₂ dating, about 150–250 g of selected ice-wedge sample was cut into 15–25 small pieces for gas extraction using the SNU dry extraction system. The gas extraction and gas sample collection protocols were identical to those used for GHG analysis, but the extracted gas samples from 15 to 25 subsamples were collected in the same tube. The tubes were sent to Beta Analytic Inc. for radiocarbon dating.

We found a Holocene-aged plant material in CYC-01 sample (9,130 ± 40 years before present [BP]) from our radiocarbon dating. However, the plant material was found near the upper end of the CYC outcrop, and the pictures of the CYC-01 plant samples barely show any clear plant forms compared to other ones from CYB and Syrdakh (Figure A1). In addition, the Holocene-age is not consistent with the ¹⁴C dating results of enclosed CO₂ (Table 1) as well as with the water isotope data from Cyuie samples that clearly point out the Late Pleistocene age.²³ Therefore, we cannot exclude potential contamination by younger organic materials, and this datum was rejected.

3 | RESULTS

3.1 | Age and forming mechanism of ice wedges

The ¹⁴C dating results show that the studied ice wedges were formed during the last glacial period (Table 1). The Syrdakh and Churapcha ice wedges were likely formed between 20,970 ± 80 and 26,570 ± 160 years BP (present = 1950 CE). The ages of the Cyuie ice wedges were determined to be between 18,130 ± 190 and 19,270 ± 360 years BP from ¹⁴C dating of CO₂ gas.²³ However, additional ¹⁴C dating of plant remains within ice wedges yields 14,410 ± 70 years BP, suggesting that the formation of Cyuie ice wedges might have resumed during the last glacial termination. The discrepancy of ¹⁴C age between CO₂ gas and plant remains can be caused by preaged carbon from the CO₂ source.⁴¹

The δ (N₂/Ar) and δ (O₂/Ar) of the enclosed gas reflect the origin of the ice wedges and the occurrence of microbial respiration within them.^{21,24} The δ (N₂/Ar) is a useful indicator of the occurrence of snowmelt during ice-wedge formation because of different solubilities of N₂ and Ar in the water. If an ice vein is formed by freezing

TABLE 1 Summary of radiocarbon dating results from CO₂ gas and plant remains

Site	Sample ID	Type	Conventional age (years BP)	δ ¹³ C (‰ PDB)	Reference
Cyuie	CYB	CO ₂	18,130 ± 190	-27.9	Kim et al. ²³
		Plant in ice	14,410 ± 70	-23.6	This study
		Plant in adjust sediment	22,770 ± 80	-26.9	Kim et al. ²³
	CYC	CO ₂	19,270 ± 360	NA	
Churapcha	C06	CO ₂	20,970 ± 80	-30.1	
Syrdakh	S07	CO ₂	21,380 ± 80	-30.6	
	S02	Plant in ice	26,570 ± 160	-23.3	

Note: Dating results of Cyuie ice wedges from CO₂ and plant residue in the surrounding soil are adapted from Kim et al.²³ The δ¹³C-CO₂ results were measured in selected samples separately to the radiocarbon analysis. NA denotes “not available” because of a lack of analysis. Abbreviations: BP, before present; PDB, Pee Dee bele.

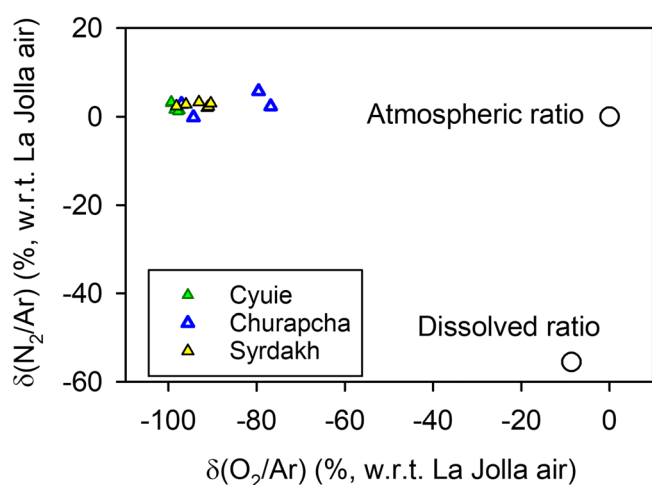


FIGURE 3 Molar ratios of N₂-O₂-Ar from the studied ice-wedge sites (Tables A1 to A3). The atmospheric ratio (upper open circle) is set to 0% by definition of δ(N₂/Ar) and δ(O₂/Ar), and the dissolved ratio (lower open circle) is a theoretical value adapted from Utting et al.⁴² The Cyuie data include the results of Kim et al.²³ [Colour figure can be viewed at [wileyonlinelibrary.com](https://onlinelibrary.wiley.com)]

meltwater, the dissolved gas in meltwater has a depleted δ(N₂/Ar) value relative to that of the atmosphere. In contrast, no dissolution occurs during the snow compaction or hoarfrost accretion, and therefore δ(N₂/Ar) does not change. As most of the ice wedges are formed below the active layer, melting and refreezing of ice wedges during preservation is unlikely. The δ(N₂/Ar) of the ice-wedge gas ranges from -10% to +6% with regard to modern air (Figure 3, Tables A1 to A3), indicating that the studied ice wedges were created more likely by dry snow compaction or hoarfrost growth rather than by snowmelt infilling into the frost cracks. All of the δ(O₂/Ar) results were lower than -75% and lower than -94% if two Churapcha samples are excluded, implying that O₂ is highly depleted within the ice wedges. The depletion of O₂ is evidence of in situ O₂ consumption by microbial respiration²⁴ and oxidation of other reduced soil materials.

3.2 | GHG mixing ratios in ice wedges

The CO₂, CH₄, and N₂O mixing ratios from the four ice wedges all showed different ranges. There were large differences among the Siberian ice wedges despite the proximity of locations (Figures 4 and 5). From all four ice wedges presented in this study, CO₂ was highly enriched compared to atmospheric mixing ratios of 170–300 ppm during the last 800,000 years recovered from polar ice cores.⁴³ The Churapcha, Cyuie, and Syrdakh ice wedges showed CO₂ mixing ratios of 8.2%–13.8%, 7.4%–13.2%, and 0.0%–10.7%, respectively. CH₄ also showed higher mixing ratios than the modern and past atmosphere. The ice-core CH₄ measurements reveal that the atmospheric CH₄ mixing ratio ranges from ~0.4 (glacial) to ~0.7 ppm (interglacial) over the past 800,000 years.⁴⁴ The Cyuie samples had an overall higher CH₄ of 11.0–91.2 ppm than the Churapcha and Syrdakh ice wedges, showing 1.3–22.5 and 1.3–10.1 ppm, respectively. Most of the N₂O compositions exhibited higher mixing ratios than the past atmospheric levels of 160–280 ppb over the past 800,000 years.⁴⁵ However, three samples from Cyuie ice wedges showed N₂O mixing ratios within, or lower than, past atmospheric variations. Churapcha ice wedges showed the highest N₂O mixing ratio among the Siberian ice wedges, ranging from 1.45 to 141.40 ppm, while Cyuie and Syrdakh ice wedges exhibited 0.01–5.46 (excluding the results below the detection limit) and 0.06–16.88 ppm, respectively. Next, we discuss the origin of each GHG.

4 | DISCUSSION

4.1 | Origin of the GHG in ice wedges

4.1.1 | CO₂

The observed CO₂ mixing ratios are best explained by in situ microbial respiration, which produces CO₂ while consuming O₂. The carbon stable isotope ratio of CO₂ (δ¹³C-CO₂) measured simultaneously with gas-phase radiocarbon dating (see Section 2.5) ranges from -30.6‰

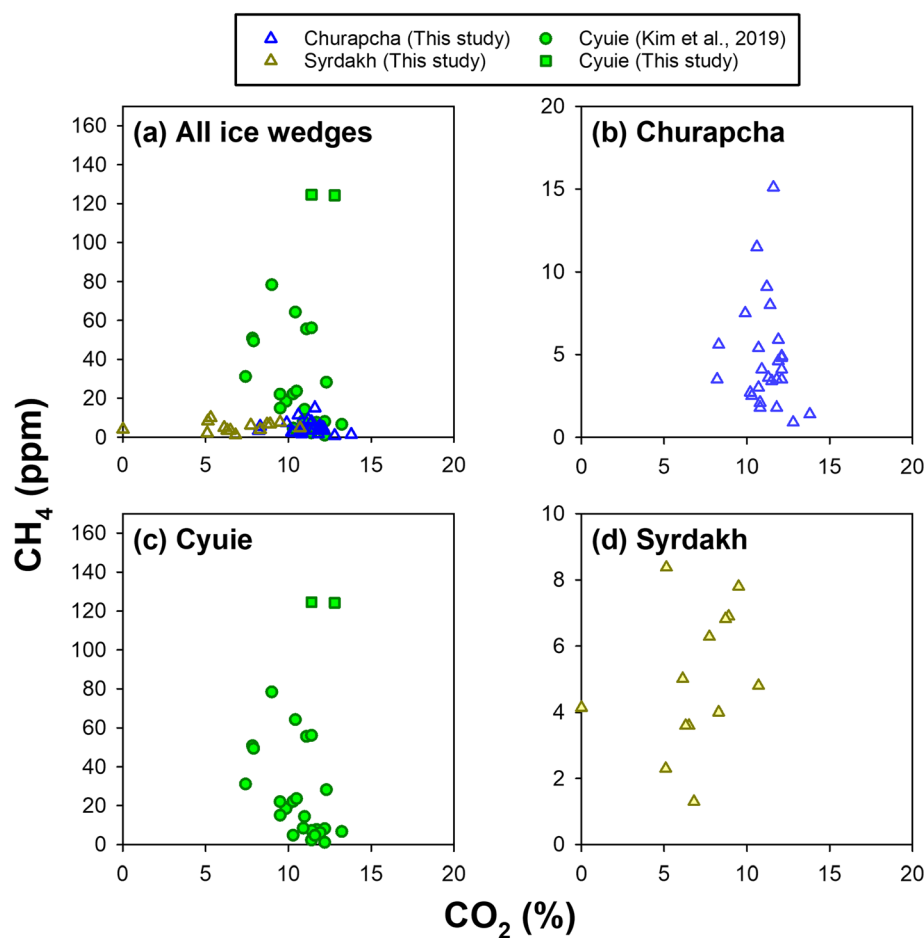


FIGURE 4 CO₂ and CH₄ mixing ratios from (a) all the ice wedges studied in this research, (b) Churapcha, (c) Cyuiie, and (d) Syrdakh sites [Colour figure can be viewed at wileyonlinelibrary.com]

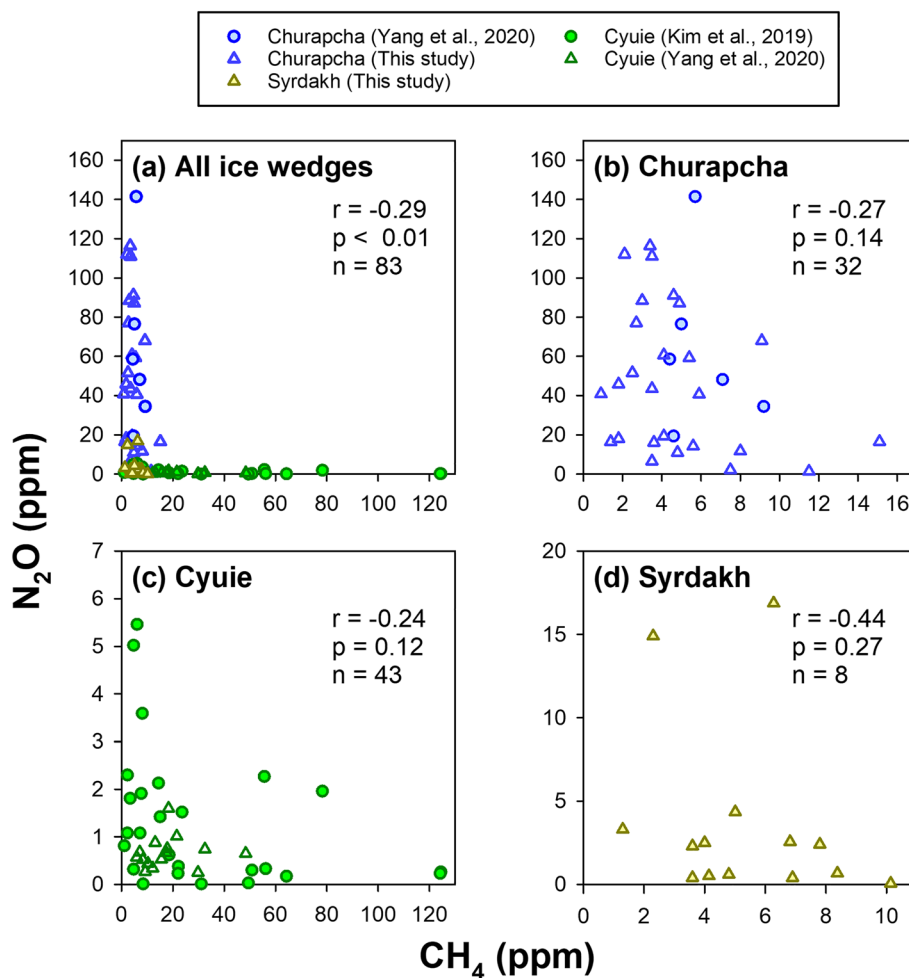
to -27.9% , with a mean of -29.5 ± 1.2 (1σ)‰ (Table 1). This implies that most of the CO₂ in studied ice wedges was produced by microbial respiration, which is consistent with the depleted $\delta(\text{O}_2/\text{Ar})$ (Figure 3). Due to the high solubility of CO₂, refreezing snow meltwater during the ice-wedge formation can increase the CO₂ composition by up to $\sim 2\%$.^{20,46} In addition, during refreezing, low diffusivity of CO₂ compared to N₂ and O₂ could enrich CO₂ composition by a factor of ~ 1.6 .²⁰ However, the $\delta(\text{N}_2/\text{Ar})$ data show no supporting evidence for snowmelt during the ice-wedge formation (Figure 3). We also did not observe textural indicators for melting after ice-wedge formation, such as disturbed foliations and elongated gas bubbles. On the contrary, CO₂ could be degassed by freezing the CaCO₃-supersaturated solution.⁴⁶ However, this was not the case, given that no evidence of partial melting and refreezing was observed.

4.1.2 | CH₄

The observed CH₄ mixing ratios were higher than the atmospheric values. Candidates for the in situ CH₄ production mechanism include snow/ice melting, abiotic (thermogenic) production, and methanogenesis. Abiotic CH₄ production is unlikely because most abiotic methanogenic reactions require higher temperatures (normally at least 25°C) than the subfreezing temperature of ice wedges.⁴⁷ The North

Greenland Eemian Ice Drilling (NEEM) ice-core records showed that the mean atmospheric CH₄ over 20,000–40,000 years BP is 453 ppb.⁴⁸ Assuming an equilibrium between air and snow/ice meltwater, the CH₄ mixing ratio in refrozen ice could increase up to three times that of the atmospheric level,⁴⁹ yielding ~ 1.4 ppm CH₄. All ice-wedge samples analyzed in this study showed a CH₄ concentration higher than 1.4 ppm, except for four samples; therefore, snowmelt during the ice-wedge formation is not the dominant mechanism of in situ CH₄ enrichment. To examine this more rigorously, we analyzed five additional ice samples from the Syrdakh site to simultaneously measure the N₂–O₂–Ar compositions with GHG mixing ratios to avoid the ice inhomogeneity problem (Table A3). All five samples exhibited CH₄ mixing ratios ranging from 4.1 to 8.4 ppm, all higher than 1.4 ppm, with $\delta(\text{N}_2/\text{Ar})$ values close to 0‰, ranging from approximately 2% to 3% with regard to modern air (Table A3). These results further support the aforementioned conclusion that snowmelt during the ice-wedge formation is not the main cause of the enriched CH₄ mixing ratios up to the order of 10⁴ ppm. Instead, the $\delta(\text{O}_2/\text{Ar})$ values of these five samples are all below -90% with regard to modern air, implying a nearly anoxic environment, which is a favorable condition for methanogenesis. Although microbial sequencing studies have not been conducted in our samples, previous studies have successfully isolated methanogenic archaea from ice wedges from Siberia and Canadian high arctic regions.^{50,51} In addition, Katayama et al.⁵²

FIGURE 5 CH₄ and N₂O from (a) all the ice wedges from central Yakutian ice wedges. The results of individual sites are plotted in (b) Churapcha, (c) Cyuie, and (d) Syrdakh [Colour figure can be viewed at wileyonlinelibrary.com]



reported a well-depleted $\delta^{13}\text{C}$ of CH₄ (−84.7‰) from an ice wedge in the Fox Tunnel, Alaska. Therefore, the previous evidence suggests that the in situ production by methanogens is the most plausible source of ice-wedge CH₄. However, considering the limited number of $\delta(\text{O}_2/\text{Ar})$ data, we cannot rule out the possibility of local aerobic conditions, as reported by St-Jean et al.²¹ and Boereboom et al.,²⁰ who found less-depleted $\delta(\text{O}_2/\text{Ar})$ ratios in different ice wedges from Alaska and northern Siberia, respectively.

4.1.3 | N₂O

Unlike CO₂ and CH₄, the ice-wedge N₂O compositions were both higher and lower than the atmospheric mixing ratios, implying that both N₂O production and consumption occurred. In natural soils, N₂O is mainly produced via nitrification and denitrification. In brief, nitrification is a series of oxidative reactions converting NH₄⁺ to NO₃[−], with intermediate substances of hydroxylamine (NH₂OH) and nitrite (NO₂[−]).⁵³ Nitrification is a strictly aerobic process because the oxidation of NH₄⁺ (to NO₂[−]) and NO₂[−] (to NO₃[−]) requires O₂ as an electron acceptor. Although N₂O is not a direct product of NH₄⁺ oxidation, significant N₂O emission by nitrification has been observed, especially under low O₂ conditions.^{54,55} N₂O is produced either by

the oxidation of NH₂OH to NO₂[−] by ammonia- and methane-oxidizing microbes⁵⁶ or by the reduction of NO₂[−] by ammonia-oxidizing bacteria.⁵⁷ The N₂O production via NO₂[−] reduction, also known as nitrifier-denitrification, increases as O₂ partial pressure decreases because NH₄⁺ oxidizing bacteria are forced to utilize NO₂[−] as an electron acceptor under O₂-limited conditions.⁵⁸ However, nitrification is completely ceased in strict anoxic conditions.⁵⁸ Denitrification is a reduction pathway of NO₃[−] to N₂, where N₂O is emitted as an intermediate product of the reduction of NO₂[−] and nitric oxide (NO). In the same manner, N₂O is also reduced to N₂ during denitrification. In contrast to nitrification, denitrification occurs in both aerobic and anaerobic conditions because denitrifying microbes utilize NO₃[−] as an electron acceptor. Soil incubation studies demonstrated that, under O₂-limited stress conditions, most of N₂O production can be attributed to denitrification and nitrifier-denitrification,^{59,60} and once a complete anoxic condition is reached, N₂O is mostly produced by denitrification.⁶⁰ Given these evidences, we can expect that the denitrification and nitrifier-denitrification were dominant N₂O producing pathways during low-O₂ period, after which denitrification has become dominant as an anoxic condition is established, until NO₃[−] is completely depleted.

Other N₂O production pathways of aerobic denitrification⁶¹ and dissimilatory nitrate reduction to ammonia (DNRA) have also been

proposed.⁶² However, the optimal temperature range (25–37°C,⁶³) for aerobic denitrification is far higher than the subfreezing temperature in buried ice wedges. The N₂O production via DNRA is considered to be minor relative to heterotrophic denitrification.⁶² Therefore, the two aforementioned mechanisms are unlikely to be major N₂O production pathways.

As mentioned earlier, some samples from the Cyuie site exhibited N₂O mixing ratios similar to or lower than the past atmosphere, which requires an in situ N₂O consuming process. A likely candidate is N₂O reduction to N₂ via denitrification. The activity of the N₂O-reducing enzyme is known to be affected by temperature^{64,65} and soil pH.^{66,67} Laboratory incubation experiments indicated that the rates of N₂O reduction are more sensitive to decreasing temperatures than N₂O production rates.^{64,65} Therefore, the subfreezing temperatures of ice wedges are not favorable for N₂O reduction to N₂. Meanwhile, the activity of N₂O-reducing enzyme is inhibited by low pH⁶⁸; that is, more N₂O is reduced to N₂ under higher pH conditions.⁶⁶ The pH measurements of the meltwater samples indicated neutral pH ranges (Tables A4 to A6). The neutral pH condition is suitable for N₂O reduction and may compensate for the inhibitory effect of subfreezing temperature. Therefore, we infer that N₂O can be reduced to N₂ within ice wedges. However, it should be noted that the pH of the liquid in the veins between ice crystals and/or thin films around soil inclusions where the microbes habitat and metabolize could be lower (i.e., more acidic) than the bulk pH. A laboratory observation using synthetic ice samples revealed that these microenvironments could be extremely acidic (pH as low as 1) due to concentrated ions in small volumes.⁶⁹ It is far beyond the scope of this study to precisely estimate the pH within these habitats and to quantify the extent to which N₂O is reduced to N₂.

There are a number of abiotic N₂O production pathways, including the dissolution of atmospheric N₂O, chemodenitrification, and the oxidation of hydroxylamine (NH₂OH). First, refreezing snowmelt during ice-wedge formation causes an elevated N₂O mixing ratio. However, here we consider the snowmelt freezing to be unlikely, considering the available δ(N₂/Ar) data and the cold climate during the Late Pleistocene. Partial melting after ice-wedge formation is also unlikely as we found no evidence of partial melting, such as elongated bubbles, glassy surfaces, or disturbed foliation.

The chemical decomposition of NH₂OH has been recognized as an important abiotic N₂O source.^{70,71} NH₂OH is produced during the first step of nitrification but is hardly detectable in soils because of its high reactivity.⁷² NH₂OH is chemically oxidized with the reduction of ferric iron (Fe³⁺) or manganese (IV).⁷³ The chemical oxidation of NH₂OH occurs predominantly in acidic conditions because, at higher pH, unprotonated NH₂OH reacts with soil organic matter rather than with Fe³⁺ and Mn⁴⁺ to produce N₂O.^{74–76} Without any decisive evidence, we speculated that N₂O production by chemical oxidation of NH₂OH is minor, considering that nitrification was not as dominant as denitrification in a near-anoxic environment (Figure 3), and the pH of meltwater samples from the central Yakutian ice wedges indicates neutral or slightly alkaline ranges (Tables A4 to A6).

However, the actual pH within the ice veins or thin films around the soil particles can be lower than that measured in meltwater. Future analysis of site-specific (SP) nitrogen isotopic (¹⁵N/¹⁴N) signatures of N₂O trapped in ice wedges may help us discriminate abiotic chemodenitrification from the other N₂O production pathways, as it is characterized by a distinctive SP value of 0.7 ± 6.5‰, while NH₂OH oxidation shows a much-elevated SP value of around 30‰.⁷³

Chemodenitrification is the chemical reduction of NO₃⁻ (and its reduced forms) by reaction with ferrous iron (Fe²⁺).⁷⁷ N₂O production by abiotic chemodenitrification has been observed in Antarctic lakes (Lake Vida and Don Juan Pond) under cold, high Fe, and saline environments^{78,79} where the dark, subzero temperature environments are similar to buried ice wedges. Chemodenitrification prefers NO₂⁻ over NO₃⁻ to produce N₂O and N₂.^{78,79} Although no NO₂⁻ data are available, most ice-wedge samples show low NO₃⁻ concentrations, with six samples showing below the detection level of 0.01 mg/L (Table 2). If chemodenitrification is the sole pathway, NO₂⁻ should be depleted rather than NO₃⁻. The overall depletion of NO₃⁻ in the studied ice wedges cannot be explained without microbial denitrification. On the contrary, Fe²⁺ is essential for chemodenitrification to reduce NO₂⁻ abiotically. Lake Vida brine is enriched in Fe (307.9 ± 22.6 μmol L⁻¹).⁸⁰ In contrast, dissolved chemistry analysis of the porewaters and interstitial ice in the upper peat layers from the Western Siberian Lowland demonstrates an order of magnitude lower Fe concentration (0.68 and 2.05 mg L⁻¹ for peat porewater and peat ice, respectively) than that reported in Lake Vida.^{80,81} This

TABLE 2 Summary of major ion concentrations of ice-wedge meltwater samples where the GHG compositions were measured at the adjacent ice

Ion	F ⁻ (mg L ⁻¹)	Cl ⁻ (mg L ⁻¹)	NO ₃ ⁻ (mg L ⁻¹)	NH ₄ ⁺ (mg L ⁻¹)	PO ₄ ³⁻ (mg L ⁻¹)	SO ₄ ²⁻ (mg L ⁻¹)	Ca ²⁺ (mg L ⁻¹)	Mg ²⁺ (mg L ⁻¹)	Na ⁺ (mg L ⁻¹)	K ⁺ (mg L ⁻¹)
Churapcha (n = 17)	0.2 ± 0.1	2.7 ± 0.6	0.4 ± 0.4	1.5 ± 0.3	0.1 ± 0.0	6.7 ± 9.7	10.4 ± 3.8	6.8 ± 1.7	3.4 ± 1.1	1.4 ± 0.3
Cyuie (n = 7)	0.1 ± 0.0	48.3 ± 76.6	0.0 ± 0.0	2.6 ± 0.9	0.0 ± 0.0	2.47 ± 0.8	6.8 ± 0.4	3.9 ± 1.2	34.5 ± 53.7	1.7 ± 0.7
Syrdakh (n = 6)	0.1 ± 0.1	2.0 ± 0.9	0.6 ± 0.6	1.5 ± 0.4	0.2 ± 0.0	1.24 ± 0.6	9.4 ± 1.8	6.3 ± 1.5	1.7 ± 0.8	1.4 ± 0.2

Abbreviation: GHG, greenhouse gas.

observation implies that the chemodenitrification in ground ice is possibly much weaker than that in the isolated lakes in Antarctica. Finally, another difference from the Antarctic lakes is that the wedge ice is preserved in subfreezing temperatures. Under a frozen state, the H₂O availability for chemodenitrification reaction should also be limited. Considering together, we consider that the chemodenitrification may not be a sole or dominant N₂O production pathway, but we cannot rule out its occurrence. The relative proportion of N₂O produced by chemodenitrification is difficult to estimate unless additional chemical and isotopic data become available. In summary, to our best knowledge, we found no strong evidence that supports dominant abiotic N₂O production pathways.

4.2 | Relationship between CO₂ and CH₄

A key result in this study is the different ranges of CH₄ mixing ratios among ice wedges; thus, it is important to discuss potential factors controlling CH₄ production and/or consumption. Previous studies have reported negative correlations between the CO₂ and CH₄ mixing ratios from different ice wedges,^{23,25} attributed to aerobic CH₄ oxidation.²⁵ In contrast, our results do not support this, as none of the ice wedges in this study exhibited a significant negative correlation between CO₂ and CH₄ mixing ratios. Rather, they had similar ranges of CO₂ mixing ratios, while the CH₄ ranges were more varied (Figure 4). Aerobic CH₄ oxidation to CO₂ occurs in the presence of O₂, which effectively inhibits anoxic methanogenesis, but CO₂ production via aerobic respiration continues, such that CH₄ continuously decreases while CO₂ increases via microbial respiration and CH₄ oxidation. Therefore, the CH₄ oxidation may lead to a negative correlation between CO₂ and CH₄ under the presence of O₂. However, in the absence of O₂, methanogenesis becomes active, and the pattern of production/consumption of CH₄ and CO₂ depends on methanogenesis pathways. Acetoclastic methanogens convert 1 mole of acetate (CH₃COOH) into 1 mole of CO₂ and CH₄. Instead, hydrogenotrophic methanogens use H₂ as an electron donor to reduce CO₂ into CH₄ and H₂O.⁸² The relative proportions of these two pathways show a large difference between study regions. For example, acetoclastic methanogenesis is predominant in arctic and subarctic permafrost soils in northwestern Siberia,⁸³ while hydrogenotrophic methanogenesis prevails in nutrient-poor boreal peatlands in Finland because of limited acetate production.⁸⁴ Our observation indicating any significant (neither positive nor negative) correlation suggests that both methanogenic pathways occurred together.

CH₄ oxidation is also observed in anaerobic environments;^{85,86} however, CH₄ consumption by anaerobic CH₄ oxidation is mostly lower than CH₄ production by methanogenesis; approximately 0.3% of CH₄ produced was oxidized to CO₂ in Alaskan peat soils,⁸⁵ and about 11.5% by average in North American peat samples over 40 days of incubation.⁸⁶ The aforementioned evidence implies that anaerobic CH₄ oxidation (and CO₂ production) is of minor importance compared to anaerobic CH₄ production, and it is thus difficult to observe in our results.

4.3 | Relationship between CH₄ and N₂O

Our previous study found a remarkable characteristic in the distribution of the CH₄ and N₂O mixing ratios in two ice-wedge outcrops in Cyuie, central Yakutia.²³ The Cyuie CH₄ and N₂O mixing ratios exhibited a clear “L-shaped” distribution in that the ice-wedge samples enriched in CH₄ (N₂O) were depleted in N₂O (CH₄) mixing ratios. This indicates that CH₄ and N₂O cannot be enriched simultaneously; therefore, some inhibitory effects should play an important role in the CH₄⁻ and N₂O⁻ producing pathways. Here, we further explored the CH₄-N₂O relationship from different ice wedges in central Yakutia.

The CH₄ and N₂O distributions from the studied ice wedges, including the results of Kim et al.²³ and Yang et al.,²⁶ are summarized in Figure 5. All the ice wedges from three locations exhibited an L-shaped CH₄-N₂O distribution (Figure 5). Such L-shaped relationship was first observed in Cyuie;²³ therefore our observation implies that the L-shaped relationship is a common feature in ice wedges—this is one of the main findings of this study. The correlation coefficients and significance (p-value) are denoted in each panel of Figure 5, which shows weak or insignificant anticorrelations. Here, we note that the L-shaped distribution is not identical to the anticorrelation. Thus, the weak anticorrelations do not contradict our findings.

The L-shaped distribution is best explained by the inhibitory effect on methanogenesis by NO₃⁻ and its denitrification products, that is, NO₂⁻, NO, and N₂O.⁸⁷⁻⁸⁹ Two mechanisms for the inhibition of methanogenesis have been proposed: competition for hydrogen (H₂) and toxic effects. Klüber and Conrad⁸⁸ observed that the addition of NO₃⁻, NO₂⁻, NO, and N₂O to soil slurries resulted in a decrease in H₂ partial pressure because denitrifying microbes utilize H₂ more effectively than methanogens. In parallel, the authors also observed an increase in ferric (Fe [III]) and sulfate ions, which can be used by Fe and sulfate-reducing bacteria that further outcompete methanogens. However, the competition for H₂ alone cannot fully explain the observed L-shaped relationship for the following reasons. First, inhibition by H₂ competition only affects hydrogenotrophic methanogenesis,⁸⁸ and thus the acetoclastic methanogens should be unaffected. Furthermore, if competition for H₂ is the dominant mechanism affecting methanogenesis, CH₄ production should have been resumed once most of the alternative electron acceptors for denitrification (such as NO₃⁻ and SO₄²⁻) are oxidized or, in other words, once the competition for H₂ is lifted. In such cases, methanogenesis follows N₂O production, and as a consequence, both CH₄ and N₂O concentrations should be elevated. However, this is not supported by our observations that show clear L-shaped patterns (Figure 5).

Instead, the toxic effect of methanogens might have a wider and more irreversible effect. Klüber and Conrad⁸⁸ found that CH₄ production rates resumed after exposure to NO₃⁻, NO₂⁻, NO, and N₂O were lower than those in untreated control soils. In addition, Klüber and Conrad⁸⁹ observed that the effects of exposure to NO and N₂O were reversible only under certain conditions depending on the concentrations of NO and N₂O and the types of methanogens tested. In this case, even after the toxic effect and/or H₂ competition is finished, the

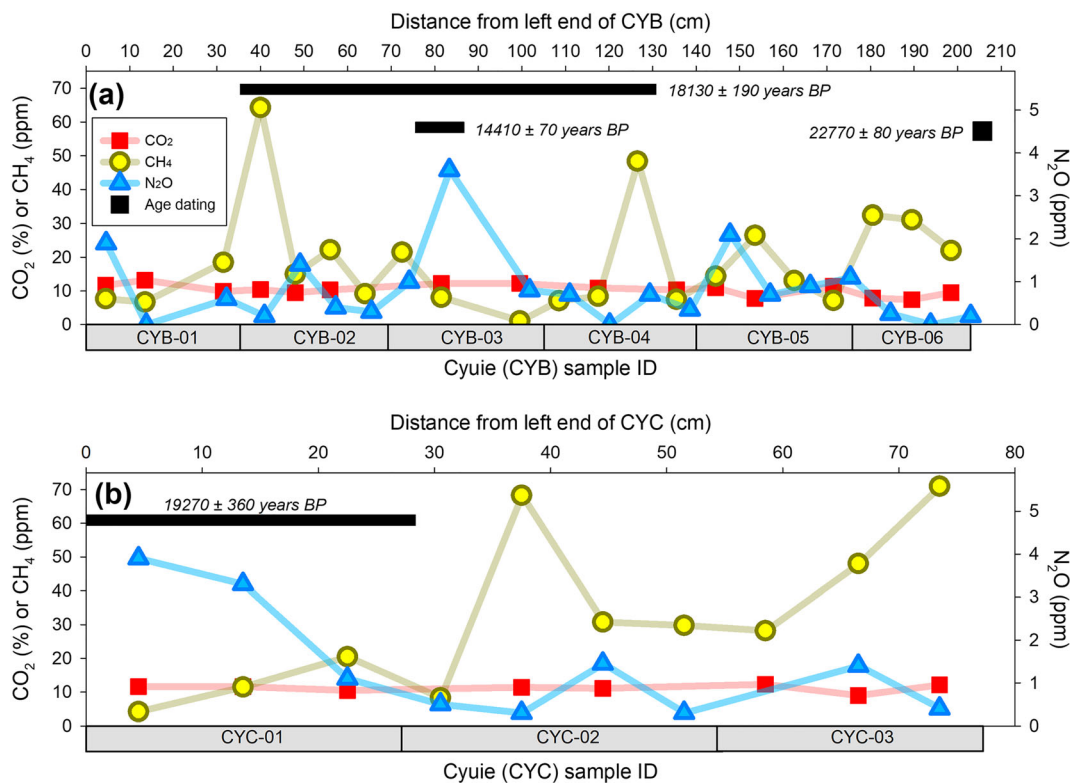


FIGURE 6 Spatial greenhouse gas distribution of (a) CYB and (b) CYC ice wedges of Cyuie site. The upper x-axis denotes the distance (in centimeters) from the left end of each ice wedge, and corresponding sample IDs are also labeled. Thick black horizontal bars indicate the sample intervals used for radiocarbon age dating [Colour figure can be viewed at [wileyonlinelibrary.com](https://onlinelibrary.wiley.com/doi/10.1002/joc.2176)]

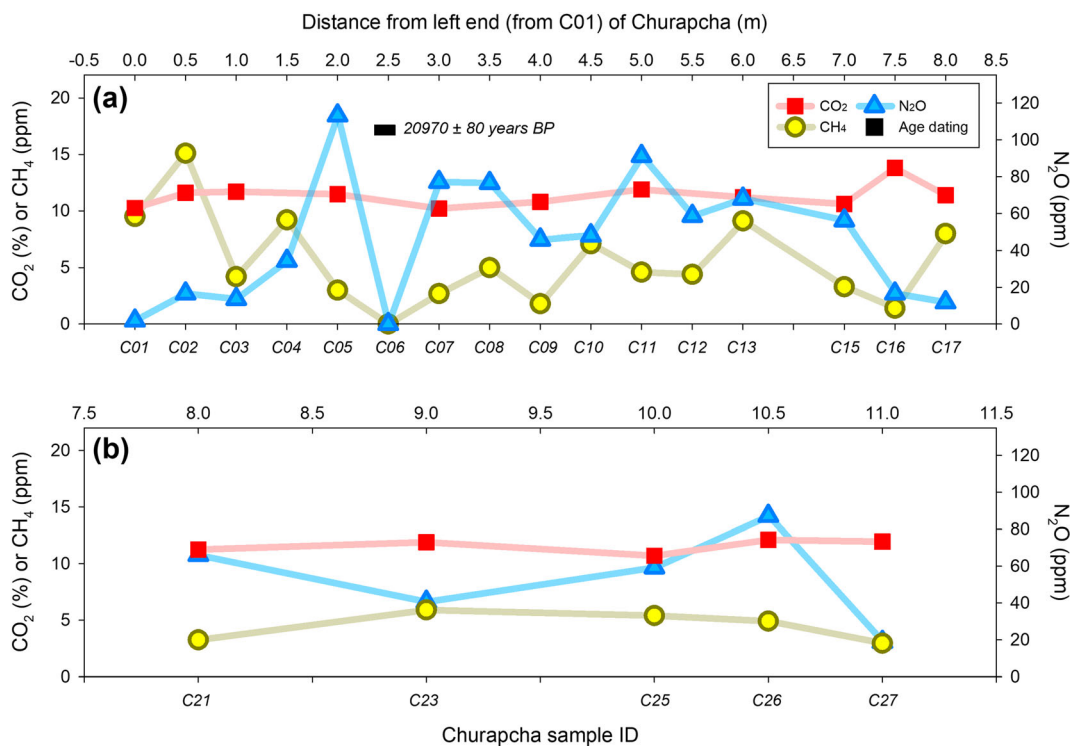


FIGURE 7 Spatial greenhouse gas distribution of two horizontal sections of (a) C01 to C17 and (b) C21 to C27 of Churapcha site. The upper x-axis denotes the distance (in centimeters) from the C01 drilling location, and corresponding sample IDs are labeled. A thick black horizontal bar indicates the sample interval used for radiocarbon age dating [Colour figure can be viewed at [wileyonlinelibrary.com](https://onlinelibrary.wiley.com/doi/10.1002/joc.2176)]

CH₄ production rate is reduced, resulting in a lower CH₄ concentration. Therefore, we consider the toxic effect as a better explanation for the observed CH₄-N₂O pattern, in particular, for the samples where the CH₄ mixing ratio is decreased (“high-N₂O-low-CH₄ samples”).

However, the inhibitory (toxic or competition) effect on methanogenesis provides no clue to the control of N₂O because denitrification occurs before methanogenesis, according to the redox sequence. There are two possible explanations for the low-N₂O-high-CH₄ samples: (i) stronger N₂O reduction to N₂ or (ii) lower initial availability of NO₃⁻ and its denitrification products compared to the high-N₂O-low-CH₄ samples. However, the former scenario alone cannot explain the low-N₂O-high-CH₄ patterns because the toxic effect is known to have a sustained impact on methanogenic bacteria.^{88,89} Therefore, it is more likely that the low-N₂O-high-CH₄ samples in each ice wedge initially contained fewer N-compounds (including NH₄⁺, NO₃⁻, and other intermediate products of nitrification and denitrification that can be transformed to N₂O) than the other ice-wedge samples. To the best of our knowledge, none of the scenarios can be tested because we have no measure of the initial content of the N-compounds, precise pH status within the wedge ice, or age of the individual samples.

4.4 | Spatial distribution of GHGs

The spatial distribution of GHGs can provide useful insight into the potential influence of the host sediments. If this is a dominant mechanism, the sediment-ice gas exchange may cause the GHG concentrations in the older ice to be different from those in the younger ice, because the outermost ice has been in contact with the host sediment at a large area since the first formation of ice wedges if the GHG concentrations in wedge ice and the host sediment are significantly different. The GHG concentrations in host sediment can be either lower or higher than those in wedge ice. For example, a recent study conducted in central Yakutia found that CH₄ concentrations in wedge ice are more enriched or depleted than the surrounding sediments depending on the studied sites.^{20,90}

The horizontal distributions of Churapcha and Cyuie sites commonly show that CO₂ concentrations are relatively stable (less scattered) and that CH₄ concentrations are depleted where N₂O is enriched and vice versa (Figures 5, 6, and 7), although this relationship is less clear in Churapcha (Figure 7) compared to Cyuie (Figure 6). However, we found any evidence of significant trends near the host sediments. For CH₄, in the Churapcha site, C01, C02, and C17 samples show higher CH₄ than C05, C06, and C07 that are located in the more central part, but such trend is not observed in C21–C27 samples. For N₂O, the outer samples (C01–C03, C16–C17, and C27) are generally more depleted than the other ones (Figure 7). However, these features are not seen in Cyuie and Syrdakh sites. In Cyuie, CYB-06 samples show higher CH₄ than inner samples of CYB-03, CYB-04 (except for a spike of CYB-04-C), and CYB-05, but CYB-01 samples do not. Similarly, while CYC-03 sample demonstrates a gradual increase in CH₄ toward the host sediment, CYC-01 shows a gradual

decreasing trend toward the sediment. The Cyuie N₂O results show that the nearest samples at the ice-wedge boundaries at each side (left or right) exhibit different trends in N₂O concentration (Figure 6). In the Syrdakh site, the samples located at the center of the outcrop (S02 and S05) show higher CH₄ and lower N₂O on average than the outer samples (S03, S04, S06, S07, and S08). This is the opposite trend of what is observed from the Churapcha C01–C17 samples where the central samples show lower CH₄ and higher N₂O compared to the outer part.

However, the lack of a clear signal does not mean the negligible or absence of ice-sediment exchange. The muted signal of gas exchange at ice-wedge-sediment boundaries can be resulted from any combination of the following reasons. First, the gas diffusion through the ice matrix is slow. Simulation of CO₂ and CH₄ diffusion through ice matrix revealed that the gas molecular diffusion has limited effects within ~10 cm for 18,000 years.²³ Second, under our sampling and data resolution, any alteration signal of ~10 cm scale can hardly be captured. The outermost samples in Churapcha and Syrdakh sites are at least ~10 to 30 cm apart from the host sediments. The Cyuie subsamples were cut and measured in 7 to 9 cm intervals.^{23,26} Third, the gas concentrations in the host sediments are inhomogeneous so that the GHG concentrations at each side of wedge ice can be different. Therefore, at this moment, it is difficult to estimate the exchange effect quantitatively from our current data.

4.5 | Causes of differences in CH₄ and N₂O ranges in different ice wedges

The composite CH₄-N₂O plot shows two different distribution patterns (Figure 5). The Churapcha ice wedges exhibited N₂O mixing ratios as high as ~140 ppm, while CH₄ mixing ratios were lower than 20 ppm. In contrast, the Cyuie ice wedges showed high CH₄ compositions up to near 130 ppm, and N₂O compositions were lower than 6 ppm. Syrdakh ice wedges showed lower compositions of both CH₄ and N₂O; however, the number of samples was not sufficient to determine the overall range. Here, the question arises as to why the CH₄ and N₂O ranges are different among the ice wedges.

Following our discussion in the previous section, the lower CH₄ mixing ratios in Churapcha and Syrdakh samples compared to Cyuie ones could be a result of a stronger inhibitory effect on methanogenesis by NO₃⁻ and its denitrification products. This is supported by the higher NO₃⁻ concentrations in Churapcha and Syrdakh than in Cyuie (Table 2). Although the abundances of NO₂⁻, NO, and N₂ are unknown, enriched N₂O mixing ratios in Churapcha ice may have inhibited CH₄ production either by competition for H₂ or by a toxic effect on methanogens. A possible explanation is the different redox conditions in each ice caused by different types of organic matter included during ice-wedge formation. For example, the plant litters of shrubs and tree species generally have a higher carbon-to-nitrogen (C/N) ratio than herbs. Therefore, if a high C/N ratio organic matter is included, the soil microbes require additional nitrogen to maintain their own C/N ratio, potentially leading to a nitrate deficiency.⁹¹ The

pollen assemblage analysis from lake sediment cores from Lake Baikal (52°05'N, 105°52'E⁹²), Lake Billyakh (65°17'N, 126°47'E⁹³), and Lake Chabada (61°59'N, 129°22'E⁹⁴) demonstrated a vegetation shift from herbs to shrubs and/or tree species over 20,000 to 10,000 years BP. The radiocarbon ages of selected Cyuie ice samples are slightly younger than those of Churapcha and Syrdakh (Table 1), implying that the organic matters (plant litters) in Cyuie sites were more likely from shrubs and trees than those in Churapcha and Syrdakh sites where mostly herb species were expected to be deposited. However, here we refrain from drawing any far-going conclusions not only because the radiocarbon ages of the studied ice wedges are highly uncertain since only a few samples were dated but also because detailed pollen assemblage reconstruction close to the study sites is lacking.

Another possible mechanism for the low CH₄ in Churapcha ice is competition with sulfate-reducing organisms.^{95,96} The meltwater samples of Churapcha ice wedges exhibited higher SO₄²⁻ concentrations than those of the Syrdakh and Cyuie ice wedges (95% Student's *t*-test; *p* < 0.05) (Table 2). In addition, within the Churapcha ice, five samples with SO₄²⁻ concentrations higher than 10 mg L⁻¹ had a lower CH₄ mixing ratio than the others (Table 2 and Table A1). However, excluding the five samples with >10 mg L⁻¹, the mean SO₄²⁻ concentration decreased (3.1 ± 1.3 mg L⁻¹) and was no longer significantly higher than that of the Cyuie ice samples (*p* = 0.11). This implies that competition with sulfate-reducing organisms may have a limited impact partly because it may only affect H₂-dependent methanogenesis.^{95,96}

On the contrary, depletion in both CH₄ and N₂O mixing ratios in the Syrdakh ice wedge may have resulted from three possibilities: (i) most of the N₂O had already been reduced to N₂, (ii) N₂O had yet been sufficiently produced from denitrification of NO₂⁻ or NO, or (iii) methanogens inhabiting the Syrdakh ice were particularly sensitive to the toxic effect of N₂O. However, currently, there is no chemical or microbiological evidence to elucidate the in situ mechanisms responsible for the characteristic CH₄-N₂O distribution in the Syrdakh site. Future studies performing a detailed analysis of the intermediate products of denitrification or microbial sequencing may provide further insights into the N₂O and CH₄ concentration control in ice wedges.

5 | CONCLUSION

In this study, we presented the GHG (CO₂, CH₄, and N₂O) mixing ratios enclosed in the bubbles of multiple ice wedges from central Yakutia using a precise methodology combining gas extraction, analysis, and correction, as recently established in SNU.²⁶ Together with the chemical analysis of the meltwater of the studied ice wedges, we discussed the origin and possible mechanisms of in situ production and consumption of GHG within ice wedges. The main findings of this study are as follows:

1. The CO₂ and CH₄ mixing ratios in the studied ice wedges cannot be fully explained without in situ microbial production through

aerobic respiration and methanogenesis, respectively. Meanwhile, the observed N₂O mixing ratios require both in situ production and consumption mechanisms. From the present analysis, we consider that microbial denitrification plays an important role in both N₂O production and consumption although our results provide no strong evidence to rule out abiotic N₂O production pathways.

2. Our results do not support the negative correlation between CO₂ and CH₄ mixing ratios reported in previous studies.^{23,25} Nonetheless, the lack of CO₂-CH₄ negative correlation does not mean the cessation of CH₄ oxidation to CO₂. Currently we have no proof that rules out the aerobic and/or anaerobic CH₄ oxidation occurring together with methanogenesis, and the CH₄ oxidation might decrease a portion of CH₄ produced by methanogenesis. However, the contribution of CH₄ oxidation in the production of CO₂ appears to be minor.
3. Our results show a clear “L-shaped” distribution between CH₄ and N₂O mixing ratios from three different ice wedges in the central Yakutia, implying that this relationship previously observed in Cyuie ice wedges²³ might be a more general feature than a site-specific one. The “L-shaped” distribution is best explained by the inhibitory effect of NO₃⁻ and its denitrification products on methanogenesis through competition for H₂ and toxic effects. The N₂O mixing ratios might be affected by the initial content of the N-compounds as well as by N₂O reduction to N₂.

ACKNOWLEDGEMENTS

We are grateful to K. Saito, A. Desyatkin, E. Byun, and H. Yoon for their contribution to ice sampling and logistics. We thank G. Lim, H. Kwak, and J. Kim for their support in laboratory works. This work was supported by the National Research Foundation of Korea (grant nos. 2018R1A5A1024958 and 2020M1A5A1110607) and Korea Ministry of Oceans and Fisheries (grant no. 1525011795).

CONFLICT OF INTEREST DISCLOSURE

The authors declare no conflict of interest.

PERMISSION TO REPRODUCE MATERIAL FROM OTHER SOURCES

Reproduction of figures in Yang et al.²⁶ is permitted by Creative Commons Attribution 4.0 License.

DATA AVAILABILITY STATEMENT

All the data produced in this paper are available in the main text or in Appendix A.

ORCID

Ji-Woong Yang  <https://orcid.org/0000-0001-8397-9274>

Jinho Ahn  <https://orcid.org/0000-0003-2280-2832>

Go Iwahana  <https://orcid.org/0000-0003-4628-1074>

Ji-Hoon Kim  <https://orcid.org/0000-0003-2430-3869>

Kyungmin Kim  <https://orcid.org/0000-0003-3010-2684>

Alexander Fedorov  <https://orcid.org/0000-0002-4016-2149>

REFERENCES

- Hugelius G, Strauss J, Zubrzycki S, et al. Estimated stocks of circum-polar permafrost carbon with quantified uncertainty ranges and identified data gaps. *Biogeosciences*. 2014;11(23):6573-6593. doi:10.5194/bg-11-6573-2014
- Salmon VG, Schadel C, Bracho R, et al. Adding depth to our understanding of nitrogen dynamics in permafrost soils. *J Geophys Res*. 2018;123(8):2497-2512. doi:10.1029/2018JG004518
- Schuur EAG, McGuire AD, Schädel C, et al. Climate change and the permafrost carbon feedback. *Nature*. 2015;520(7546):171-179. doi:10.1038/nature14338
- Voigt C, Marushchak ME, Lamprecht RE, et al. Increased nitrous oxide emissions from Arctic peatlands after permafrost thaw. *Proc Natl Acad Sci U S A*. 2017;114(24):6238-6243. doi:10.1073/pnas.1702902114
- Schirmermeister L, Froese D, Tumskey V, Grosse G, Wetterich S. Yedoma: Late Pleistocene ice-rich syngenetic permafrost of Beringia. In: Elias SA, ed. *The encyclopedia of quaternary science*. Vol.3. Amsterdam: Elsevier; 2013:542-552. doi:10.1016/B978-0-444-53643-3.00106-0
- Strauss J, Schirmermeister L, Grosse G, et al. The deep permafrost carbon pool of the Yedoma region in Siberia and Alaska. *Geophys Res Lett*. 2013;40:6165-6170. doi:10.1002/2013GL058088
- Strauss J, Schirmermeister L, Grosse G, et al. Deep yedoma permafrost: a synthesis of depositional characteristics and carbon vulnerability. *Earth Sci Rev*. 2017;172:75-86. doi:10.1016/j.earscirev.2017.07.007
- Cherburnina MY, Karaevskaya ES, Vasil'chuk YK, et al. Microbial and geochemical evidence of permafrost formation at Mamontova Gora and Syrdakh, central Yakutia. *Front Earth Sci*. 2021;9:739365. doi:10.3389/feart.2021.739365
- Péwé TL, Journaux A, Stuckenrath R. Radiocarbon dates and late-Quaternary stratigraphy from Mamontova Gora, unglaciated central Yakutia, Siberia, USSR. *Quatern Res*. 1977;8(1):51-63. doi:10.1016/0033-5894(77)90056-4
- Popp S, Diekmann B, Meyer H, Siegert C, Syromyatnikov I, Hubberten HW. Palaeoclimate signals as inferred from stable-isotope composition of ground ice in the Verkhoyansk foreland, central Yakutia. *Permafrost Periglac Process*. 2006;17(2):119-132. doi:10.1002/ppp.556
- Vasil'chuk YK. Paleological permafrost interpretation of oxygen isotope composition of Late Pleistocene and Holocene wedge ice of Yakutia. *Trans (Doklady) USSR Acad Sci Earth Sci Sec*. 1988;298:56-59.
- Vasilchuk YK, Shmelev DG, Cherburnina MY, Budantseva NA, Broushkov AV, Vasilchuk AC. New oxygen isotope diagrams of Late Pleistocene and Holocene ice wedges in Mamontova Gora and Syrdakh Lake, central Yakutia. *Doklady Earth Sci*. 2019;486(1):580-584. doi:10.1134/S1028334X19050283
- Walter Anthony K, Daanen R, Anthony P, et al. Methane emissions proportional to permafrost carbon thawed in Arctic lakes since the 1950s. *Nat Geosci*. 2016;9(9):679-682. doi:10.1038/NNGEO2795
- Kanevskiy M, Shur Y, Fortier D, Jorgenson MT, Stephani E. Cryostratigraphy of late Pleistocene syngenetic permafrost (yedoma) in northern Alaska, Itkillik River exposure. *Quatern Res*. 2011;75(3):584-596. doi:10.1016/j.yqres.2010.12.003
- Strauss J, Schirmermeister L, Wetterich S, Borchers A, Davydov SP. Grain-size properties and organic-carbon stock of yedoma ice complex permafrost from the Kolyma lowland, northeastern Siberia. *Global Biogeochem Cycles*. 2012;26:GB3003. doi:10.1029/2011GB004104
- Vonk JE, Sánchez-García L, van Dongen BE, et al. Activation of old carbon by erosion of coastal and subsea permafrost in Arctic Siberia. *Nature*. 2012;489(7414):137-140. doi:10.1038/nature11392
- Meredith M, Sommerkorn M, Cassotta S, et al. Polar regions. In: Pörtner H-O, Roberts DC, Masson-Delmotte V, et al., eds. *IPCC special report on the ocean and cryosphere in a changing climate*. IPCC; 2019.
- Lachenbruch AH. *Mechanics of thermal contraction cracks and ice-wedge polygons in permafrost*. special papers, 70. New York: Geological Society of America; 1962:69.
- Opel T, Meyer H, Wetterich S, Laepple T, Dereviagin A, Murton J. Ice wedges as archives of winter paleoclimate: a review. *Permafrost Periglac*. 2018;29:199-209. doi:10.1002/ppp.1980
- Boereboom T, Samyn D, Meyer H, Tison J-L. Stable isotope and gas properties of two climatically contrasting (Pleistocene and Holocene) ice wedges from cape Mamontov Klyk, Laptev Sea, northern Siberia. *Cryosphere*. 2013;7(1):31-46. doi:10.5194/tc-7-31-2013
- St-Jean M, Lauriol B, Clark ID, Lacelle D, Zdanowicz C. Investigation of ice-wedge infilling processes using stable oxygen and hydrogen isotopes, crystallography and occluded gases (O₂, N₂, Ar). *Permafrost Periglac Process*. 2011;22(1):49-64. doi:10.1002/ppp.680
- Vasil'chuk YK, Vasil'chuk AC. Radiocarbon dating and oxygen isotope variations in Late Pleistocene syngenetic ice-wedges, northern Siberia. *Permafrost Periglac Process*. 1997;8(3):335-345. doi:10.1002/(SICI)1099-1530(199709)8:3%3C335::AID-PPP259%3E3.0.CO;2-V
- Kim K, Yang J-W, Yoon H, et al. Greenhouse gas formation in ice wedges at Cyuie, central Yakutia. *Permafrost Periglac Process*. 2019;30(1):48-57. doi:10.1002/ppp.1994
- Lacelle D, Radtke K, Clark ID, et al. Geomicrobiology and occluded O₂-CO₂-Ar gas analyses provide evidence of microbial respiration in ancient terrestrial ground ice. *Earth Planet Sci Lett*. 2011;306(1-2):46-54. doi:10.1016/j.epsl.2011.03.023
- Broushkov A, Fukuda M. Preliminary measurements on methane content in permafrost, central Yakutia, and some experimental data. *Permafrost Periglac Process*. 2002;13(3):187-197. doi:10.1002/ppp.422
- Yang J-W, Ahn J, Iwahana G, Han S, Kim K, Fedorov A. Brief communication: the reliability of gas extraction techniques for analysing CH₄ and N₂O compositions in gas trapped in permafrost ice wedges. *Cryosphere*. 2020;14(4):1311-1324. doi:10.5194/tc-14-1311-2020
- Ulrich M, Grosse G, Strauss J, Schirmermeister L. Quantifying wedge-ice volumes in yedoma and thermokarst basin deposits. *Permafrost Periglac Process*. 2014;25(3):151-161. doi:10.1002/ppp.1810
- Ivanov MS. *Cryogenic composition of quaternary deposits of Lena-Aldan depression*. Siberian Branch, Novosibirsk, Russia: Nauka; 1984. (in Russian).
- Soloviev P. *Guidebook: Alas thermokarst relief of central Yakutia*. Second International Conference on Permafrost, 1973. Yakutsk: USSR Academy of Sciences, Section of Earth's Sciences, Siberian Division; 1973:13-28.
- Ulrich M, Matthes H, Schirmermeister L, et al. Differences in behavior and distribution of permafrost-Related Lakes in central Yakutia and their response to climatic drivers. *Water Resour Res*. 2017;53(2):1167-1188. doi:10.1002/2016WR019267
- Beer C, Fedorov AN, Torgovkin Y. Permafrost temperature and active-layer thickness of Yakutia with 0.5-degree spatial resolution for model evaluation. *Earth Syst Sci Data*. 2013;5(2):305-310. doi:10.5194/essd-5-305-2013
- Brown J, Ferrians OJ Jr, Heginbottom JA, Melnikov E. *Circum-Arctic map of permafrost and ground-ice conditions, version 2*. Boulder, CO: National Snow and Ice Data Center; 2002.
- Strauss J, Laboor S, Fedorov AN, et al. Database of ice-rich Yedoma permafrost (IRYP). *Pangaea*. 2016. doi:10.1594/PANGAEA.861733
- Bosikov NP. *Evolution of alases in central Yakutia*. Yakutsk, Russia: Permafrost Institute, Siberian Division of Russian Academy of Science; 1991:127. (in Russian).
- Shin J. *Atmospheric CO₂ variations on millennial time scales during the early Holocene*, master thesis, School of Earth and Environmental Sciences. South Korea: Seoul National University; 2014:58.
- Higaki S, Oya Y, Makide Y. Emission of methane from stainless steel surface investigated by using tritium as a radioactive tracer. *Chem Lett*. 2006;35:292-293. doi:10.1246/cl.2006.292

37. Ahn J, Brook EJ, Howell K. A high-precision method for measurement of paleoatmospheric CO₂ in small polar ice samples. *J Glaciol.* 2009; 55:499-506.
38. Ryu Y, Ahn J, Yang J-W. High-precision measurement of N₂O concentration in ice cores. *Environ Sci Technol.* 2018;52(2):731-738. doi:10.1021/acs.est.7b05250
39. Sowers T, Bender M, Raynaud D. Elemental and isotopic composition of occluded O₂ and N₂ in polar ice. *J Geophys Res.* 1989;94(D4):5137-5150. doi:10.1029/JD094iD04p05137
40. Petrenko VV, Severinghaus JP, Brook EJ, Reeh N, Schaefer H. Gas records from the West Greenland ice margin covering the last glacial termination: a horizontal ice core. *Quat Sci Rev.* 2006;25(9-10): 865-875. doi:10.1016/j.quascirev.2005.09.005
41. Yu S-Y, Shen J, Colman SM. Modeling the radiocarbon reservoir effect in lacustrine systems. *Radiocarbon.* 2007;49(3):1241-1254. doi:10.1017/S0033822200043150
42. Utting N, Lauriol B, Lacelle D, Clark I. Using noble gas ratios to determine the origin of ground ice. *Quatern Res.* 2016;85(1):177-184. doi:10.1016/j.yqres.2015.12.003
43. Bereiter B, Eggleston S, Schmitt J, et al. Revision of the EPICA dome C CO₂ record from 800 to 600 kyr before present. *Geophys Res Lett.* 2015;42(2):542-549. doi:10.1002/2014GL061957
44. Loulergue L, Schilt A, Spahni R, et al. Orbital and millennial-scale features of atmospheric CH₄ over the past 800,000 years. *Nature.* 2008;453(7193):383-386. doi:10.1038/nature06950
45. Schilt A, Baumgartner M, Schwander J, et al. Atmospheric nitrous oxide during the last 140,000 years. *Earth Planet Sci Lett.* 2010; 300(1-2):33-43. doi:10.1016/j.epsl.2010.09.027
46. Killawee JA, Fairchild IJ, Tison J-L, Janssens L, Lorrain R. Segregation of solutes and gases in experimental freezing of dilute solutions: implications for natural glacial systems. *Geochim Cosmochim Acta.* 1998;62(23-24):3637-3655. doi:10.1016/S0016-7037(98)00268-3
47. Etiope G, Sherwood Lollar B. Abiotic methane on earth. *Rev Geophys.* 2013;51(2):276-299. doi:10.1002/rog.20011
48. Chappellaz J, Stowasser C, Blunier T, et al. High-resolution glacial and deglacial record of atmospheric methane by continuous-flow and laser spectrometer analysis along the NEEM ice core. *Clim Past.* 2013; 9(6):2579-2593. doi:10.5194/cp-9-2579-2013
49. Yang J-W, Ahn J, Brook EJ, Ryu Y. Atmospheric methane control mechanisms during the early Holocene. *Clim Past.* 2017;13(9):1227-1242. doi:10.5194/cp-13-1227-2017
50. Rivkina E, Shcherbakova V, Laurinavichius K, et al. Biogeochemistry of methane and methanogenic archaea in permafrost. *FEMS Microbiol Ecol.* 2007;61(1):1-15. doi:10.1111/j.1574-6941.2007.00315.x
51. Steven B, Pollard WH, Greer CW, Whyte LG. Microbial diversity and activity through a permafrost/ground ice core profile from the Canadian high Arctic. *Environ Microbiol.* 2008;10(12):3388-3403. doi:10.1111/j.1462-2920.2008.01746.x
52. Katayama T, Tanaka M, Moriizumi J, et al. Phylogenetic analysis of bacteria preserved in a permafrost ice wedge for 25,000 years. *Appl Environ Microbiol.* 2007;73(7):2360-2363. doi:10.1128/AEM.01715-06
53. Tiedje JM. Ecology of denitrification and dissimilatory nitrate reduction to ammonium. In: Zehnder AJB, ed. *Biology of anaerobic microorganisms.* New York, USA: John Wiley & Sons; 1988:179-244.
54. Bateman EJ, Baggs EM. Contributions of nitrification and denitrification to N₂O emissions from soils at different water-filled pore space. *Biol Fertil Soils.* 2005;41(6):379-388. doi:10.1007/s00374-005-0858-3
55. Ma WK, Schautz A, Fishback LE, Bedard-Haughn A, Farrel RE, Siciliano ST. Assessing the potential of ammonia oxidizing bacteria to produce nitrous oxide in soils of a high arctic lowland ecosystem on Devon Island, Canada. *Soil Biol Biochem.* 2007;39(8):2001-2013. doi:10.1016/j.soilbio.2007.03.001
56. Sutka RL, Ostrom NE, Ostrom PH, Gandhi H, Breznak JA. Nitrogen isotopomer site preference of N₂O produced by *Nitrosomonas europaea* and *Methylococcus capsulatus* Bath. *Rapid Commun Mass Spectrom.* 2003;17(7):738-745. doi:10.1002/rcm.968
57. Yoshida T, Alexander M. Nitrous oxide formation by *Nitrosomonas europaea* and heterotrophic microorganisms. *Soil Sci Soc Am pro.* 1970;34(6):880-882. doi:10.2136/sssaj1970.03615995003400060020x
58. Wrage-Mönnig N, Horn MA, Well R, Müller C, Velthof G, Oenema O. The role of nitrifier denitrification in the production of nitrous oxide revised. *Soil Biol Biochem.* 2018;123:A3-A16. doi:10.1016/j.soilbio.2018.03.020
59. Ostrom NE, Sutka R, Ostrom PH, et al. P.: Isotopologue data reveal bacterial denitrification as the primary source of N₂O during a high flux event following cultivation of a native temperate grassland. *Soil Biol Biochem.* 2009;42(3):499-506.
60. Zhu X, Burger M, Doane TA, Horwath WR. Ammonia oxidation pathways and nitrifier denitrification are significant sources of N₂O and NO under low oxygen availability. *Proc Natl Acad Sci U S A.* 2013; 110(16):6328-6333. doi:10.1073/pnas.1219993110
61. Robertson LA, Kuenen JG. Aerobic denitrification—old wine in new bottles? *Antonie Van Leeuwenhoek.* 1984;50(5):525-544. doi:10.1007/BF02386224
62. Cole JA. Assimilatory and dissimilatory reduction of nitrate to ammonia. In: Cole JA, Ferguson SJ, eds. *The nitrogen and Sulphur cycles.* Cambridge: Cambridge University Press; 1988:281-329.
63. Ji B, Yang K, Zhu L, et al. Aerobic denitrification: a review of important advances of the last 30 years. *Biotechnol Bioprocess Eng.* 2015; 20(4):643-651. doi:10.1007/s12257-015-0009-0
64. Holtan-Hartwig L, Dörsch P, Bakken LR. Low temperature control of soil denitrifying communities: kinetics of N₂O production and reduction. *Soil Biol Biochem.* 2002;34(11):1797-1806. doi:10.1016/S0038-0717(02)00169-4
65. Maag M, Vinther FP. Nitrous oxide emission by nitrification and denitrification in different soil types and at different soil moisture contents and temperatures. *Appl Soil Ecol.* 1996;4(1):5-14. doi:10.1016/0929-1393(96)00106-0
66. Liu B, Mørkved PT, Frostegard Å, Reier Bakken L. Denitrification gene pools, transcription and kinetics of NO, N₂O and N₂ production as affected by soil pH. *FEMS Microbiol Ecol.* 2010;72(3):407-417. doi:10.1111/j.1574-6941.2010.00856.x
67. Šimek M, Cooper JE. The influence of soil pH on denitrification: progress towards the understanding of this interaction over the last 50 years. *Eur J Soil Sci.* 2002;53(3):345-354. doi:10.1046/j.1365-2389.2002.00461.x
68. Knowles R. Denitrification. *Microbiol Rev.* 1982;46:43-70.
69. Barletta RE, Roe CH. Chemical analysis of ice vein μ -environments. *Polar Rec.* 2012;48(4):334-341. doi:10.1017/S0032247411000635
70. Bremner JM. Sources of nitrous oxide in soils. *Nutr Cycl Agroecosyst.* 1997;49:7-16. doi:10.1023/A:1009798022569
71. Schreiber F, Wunderlin P, Udert KM, Wells GF. Nitric oxide and nitrous oxide turnover in natural and engineered microbial communities: biological pathways, chemical reactions, and novel technologies. *Front Microbiol.* 2012;3:372. doi:10.3389/fmicb.2012.00372
72. Heil J, Vereecken H, Brüggemann N. A review of chemical reactions of nitrification intermediates and their role in nitrogen cycling and nitrogen trace gas formation in soil. *Eur J Soil Sci.* 2016;67(1):23-39. doi:10.1111/ejss.12306
73. Zhu-Barker X, Cavazos AR, Ostrom NE, Horwath WR, Glass JB. The importance of abiotic reactions for nitrous oxide production. *Biogeochemistry.* 2015;126(3):251-267. doi:10.1007/s10533-015-0166-4
74. Liu S, Herbst M, Bol R, et al. The contribution of hydroxylamine content to spatial variability of N₂O formation in soil of a Norway spruce forest. *Geochim Cosmochim Acta.* 2016;178:76-86. doi:10.1016/j.gca.2016.01.026

75. Liu S, Berns AE, Vereecken H, Wu D, Bruggemann N. Interactive effects of MnO₂, organic matter and pH on abiotic formation of N₂O from hydroxylamine in artificial soil mixtures. *Sci Rep.* 2017;7(1):39590. doi:10.1038/srep39590
76. Thorn KA, Arterburn JB, Mikita MA. Nitrogen-15 and carbon-13 NMR investigation of hydroxylamine-derivatized humic substances. *Environ Sci Technol.* 1992;26(1):107-116. doi:10.1021/es00025a011
77. Picardal F. Abiotic and microbial interactions during anaerobic transformations of Fe (III) and NO_x⁻. *Front Microbiol.* 2012;3:1, 112-7. doi:10.3389/fmicb.2012.00112
78. Ostrom NE, Gandhi H, Trubl G, Murray AE. Chemodenitrification in the cryoecosystem of Lake Vida, Victoria Valley, Antarctica. *Geobiology.* 2016;14(6):575-587. doi:10.1111/gbi.12190
79. Samarkin VA, Madigan MT, Bowles MW, et al. Abiotic nitrous oxide emission from the hypersaline Don Juan pond in Antarctica. *Nat Geosci.* 2010;3(5):341-344. doi:10.1038/ngeo847
80. Murray AE, Kenig F, Fritsen CH, et al. Microbial life at -13°C in the brine of an ice-sealed Antarctic lake. *Proc Natl Acad Sci USA.* 2012;109:20626-20631. doi:10.1073/pnas.1208607109
81. Lim AG, Loiko SV, Kuzmina DM, et al. Dispersed ground ice of permafrost peatlands: potential unaccounted carbon, nutrient and metal sources. *Chemosphere.* 2021;266:128953. doi:10.1016/j.chemosphere.2020.128953
82. Conrad R. Contribution of hydrogen to methane production and control of hydrogen concentrations in methanogenic soils and sediments. *FEMS Microbiol Ecol.* 1999;28(3):193-202. doi:10.1111/j.1574-6941.1999.tb00575.x
83. Metje M, Frenzel P. Methanogenesis and methanogenic pathways in a peat from subarctic permafrost. *Environ Microbiol.* 2007;9(4):954-964. doi:10.1111/j.1462-2920.2006.01217.x
84. Galand PE, Yrjälä K, Conrad R. Stable carbon isotope fractionation during methanogenesis in three boreal peatland ecosystem. *Biogeochemistry.* 2010;7(11):3893-3900. doi:10.5194/bg-7-3893-2010
85. Blazewicz SJ, Petersen DG, Waldrop MP, Firestone MK. Anaerobic oxidation of methane in tropical and boreal soils: ecological significance in terrestrial methane cycling. *J Geophys Res.* 2012;112(G2):G02033. doi:10.1029/2011JG001864
86. Gupta V, Smemo KA, Yavitt JB, Fowle D, Branfireun B, Basiliko N. Stable isotopes reveal widespread anaerobic methane oxidation across latitude and peatland type. *Environ Sci Technol.* 2013;47(15):8273-8279. doi:10.1021/es400484t
87. Fischer R, Thauer RK. Methanogenesis from acetate in cell extracts of *Methanosarcina barkeri*: isotope exchange between CO₂ and the carbonyl group of acetyl-CoA, and the role of H₂. *Arch Microbiol.* 1990;153(2):156-162. doi:10.1007/BF00247814
88. Klüber HD, Conrad R. Effects of nitrate, nitrite, NO and N₂O on methanogenesis and other redox processes in anoxic rice field soil. *FEMS Microbiol Ecol.* 1998a;25(3):301-318. doi:10.1111/j.1574-6941.1998.tb00482.x
89. Klüber HD, Conrad R. Inhibitory effects of nitrate, nitrite, NO and N₂O on methanogenesis by *Methanosarcina barkeri* and *Methanobacterium bryantii*. *FEMS Microbiol Ecol.* 1998b;25(4):331-339. doi:10.1111/j.1574-6941.1998.tb00484.x
90. Cherbunina MY, Shmelev DG, Brouchkov AV, Kazancev VS, Argunov, RN. Patterns of spatial methane distribution in the upper layers of the permafrost in central Yakutia. *Mosc Univ Geol Bull.* 2018;73:100-108.
91. Weil RR, Brady NC. *The nature and properties of soils.* 15th ed. Pearson; 2017.
92. Demske D, Heumann G, Granoszewski W, et al. Late glacial and Holocene vegetation and regional climate variability evidenced in high-resolution pollen records from Lake Baikal. *Global Planet Change.* 2005;46(1-4):255-279. doi:10.1016/j.gloplacha.2004.09.020
93. Müller S, Tarasov PE, Andreev AA, Tutken T, Gartz S, Diekmann B. Late Quaternary vegetation and environments in the Verkhoyansk Mountains region (NE Asia) reconstructed from a 50-kyr fossil pollen record from Lake Billyakh. *Quat Sci Rev.* 2010;29(17-18):2071-2086. doi:10.1016/j.quascirev.2010.04.024
94. Tarasov P, Williams JW, Andreev A, et al. Satellite- and pollen-based quantitative woody cover reconstructions for northern Asia: verification and application to late-Quaternary pollen data. *Earth Planet Sci Lett.* 2007;264(1-2):284-298. doi:10.1016/j.epsl.2007.10.007
95. Abram JW, Nedwell DB. Inhibition of methanogenesis by sulphate reducing bacteria competing for transferred hydrogen. *Arch Microbiol.* 1978;117(1):89-92. doi:10.1007/BF00689356
96. Robinson JA, Tiedje JM. Competition between sulfate-reducing and methanogenic bacteria for H₂ under resting and growing conditions. *Arch Microbiol.* 1984;137(1):26-32. doi:10.1007/BF00425803

How to cite this article: Yang J-W, Ahn J, Iwahana G, et al. Origin of CO₂, CH₄, and N₂O trapped in ice wedges in central Yakutia and their relationship. *Permafrost and Periglac Process.* 2023;34(1):122-141. doi:10.1002/ppp.2176

APPENDIX A

TABLE A1 GHG mixing ratios and molar ratios of N₂-O₂-Ar from Churapcha ice wedges measured using a dry extraction technique (“dry hit5” protocol)²⁶

Sample ID	CO ₂ (%)	CH ₄ (ppm)	N ₂ O (ppm)	δ(O ₂ /Ar) (%)	δ(N ₂ /Ar) (%)	Reference
C01	10.6	11.5	1.5			This study
	9.9	7.5	2.2			
C02	11.6	15.1	16.6			This study
	12.1	4.8	11.1			
C03	11.3	3.6	16.2			This study
	n.m.	9.2	34.4			
C04	12.1	3.5	111.1			This study
	10.8	2.1	112.1			
	11.5	3.4	116.3			
C05	10.2	2.7	77.1			This study
	n.m.	5.0	76.5			
C06	10.8	1.8	45.8			This study
	n.m.	7.1	48.1			
C07	11.9	4.6	91.2			This study
	n.m.	4.4	58.6	-79.56 (this study)	5.73 (this study)	
C08	11.2	9.1	68.0			This study
	10.3	2.5	51.6			
C09	10.9	4.1	60.7			This study
	13.8	1.4	16.6	-76.82	2.32	
C10	11.4	8.0	11.8			This study
	n.m.	4.6	19.4			
C11	12.8	0.9	40.8			This study
	11.8	3.5	43.5			
C12	10.7	3.0	88.5			This study
	11.9	5.9	40.6			
C13	10.7	5.4	59.3			This study
	12.1	4.9	87.2			
C14	11.8	1.8	18.1			This study
	12.1	4.1	19.4	-94.31	-0.17	
C15	n.m.	5.7	141.4			This study
	8.2	3.5	6.6			
C16	8.3	5.6	14.3			This study

Note: “n.m.” denotes data not measured.

TABLE A2 Compilation of GHG mixing ratios and molar ratios of N₂-O₂-Ar from Cyuie ice wedges published in previous works^{23,26}

Sample ID	CO ₂ (%)	CH ₄ (ppm)	N ₂ O (ppm)	δ(O ₂ /Ar) (%)	δ(N ₂ /Ar) (%)	Reference
CYB-01-A	11.7	7.7	1.9			23
CYB-01-B	13.2	6.7	n.d.			
CYB-01-D	9.9	18.5	0.6	-98.57 (this study)	1.57 (this study)	
CYB-02-A	10.4	64.3	0.2			
CYB-02-B	9.5	15.0	1.4			
CYB-02-C	10.3	22.2	0.4			
CYB-02-D	n.m.	9.2	0.3			26
CYB-03-A	n.m.	21.5	1.0	-97.80 (this study)	1.25 (this study)	
CYB-03-B	12.2	8.1	3.6			23
CYB-03-D	12.2	1.1	0.8			
CYB-04-A	n.m.	7.1	0.7			26
CYB-04-B	10.9	8.4	0.0			23
CYB-04-C	n.m.	48.4	0.7			26
CYB-04-D	10.3	4.7	0.3			23
	n.m.	10.3	0.4			26
CYB-05-A	11.0	14.4	2.1			23
CYB-05-B	7.8	50.8	0.3			
	n.m.	2.2	1.1			
CYB-05-C	n.m.	13.1	0.9			26
CYB-05-D	11.4	7.2	1.1	-99.34 (this study)	3.31 (this study)	23
CYB-06-A	n.m.	15.5	0.5			26
	7.9	49.4	0.0			23
CYB-06-B	7.4	31.1	0.0			
CYB-06-C	9.5	22.0	0.2			
CYC-01-A	11.9	6.1	5.5			
	11.4	2.3	2.3			
CYC-01-B	11.6	4.7	5.0			
	n.m.	18.3	1.6			26
CYC-01-C	n.m.	17.4	0.7			
	10.5	23.6	1.5			23
CYC-02-A	n.m.	8.3	0.5			26
CYC-02-B	n.m.	12.1	0.3			
	11.4	124.5	0.3			23
CYC-02-C	n.m.	5.9	0.6			26
	11.1	55.7	2.3			23
CYC-02-D	n.m.	29.8	0.3			26
CYC-03-A	12.3	28.2	n.d.			23
CYC-03-B	n.m.	17.8	0.8			26
	9.0	78.3	2.0			23
CYC-03-C	11.4	56.1	0.3			
	n.m.	32.5	0.7			26
	12.8	124.3	0.2			23

Note: The data published in Kim et al.²³ were corrected for systematic blank correction following Yang et al.²⁶ "n.m." denotes data not measured, and "n.d." denotes the results below zero after correction.

Abbreviation: GHG, greenhouse gas.

Sample ID	CO ₂ (%)	CH ₄ (ppm)	N ₂ O (ppm)	δ(O ₂ /Ar) (%)	δ(N ₂ /Ar) (%)	Reference
S02	6.5	3.6	2.3			This study
	8.7	6.8	2.6	-91.20	2.04	
S03	8.3	4.0	2.6			
	0.0	4.1	0.5	-98.18	2.35	
S04	9.5	7.8	2.5			
S05	10.7	4.8	0.6			
	8.9	6.9	0.4			
	0.0	9.6	0.5	-90.91	2.30	
S06	6.8	1.3	3.3			
	5.1	2.3	14.9			
	7.7	6.3	16.9	-90.38	3.02	
S07	6.1	5.0	4.4			
S08	6.3	3.6	0.4			
	5.3	10.1	0.1			
	5.1	8.4	0.7	-93.07	3.28	

Note: "n.m." denotes data not measured.

Abbreviation: GHG, greenhouse gas.

TABLE A3 GHG mixing ratios and molar ratios of N₂-O₂-Ar from Syrdakh ice wedges measured using dry extraction technique ("dry hit5" protocol)²⁶

TABLE A4 Major ion concentrations and pH measurements from the meltwater samples of the Churapcha ice wedge

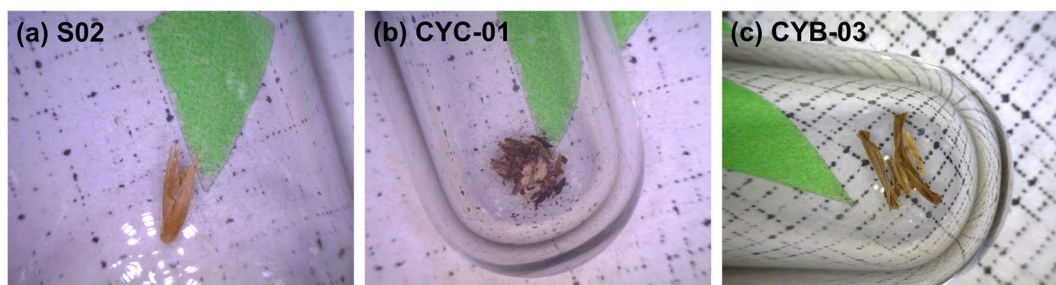
Sample ID	NH ₄ ⁺ (mg L ⁻¹)	Ca ²⁺ (mg L ⁻¹)	K ⁺ (mg L ⁻¹)	Mg ²⁺ (mg L ⁻¹)	Na ⁺ (mg L ⁻¹)	Cl ⁻ (mg L ⁻¹)	SO ₄ ²⁻ (mg L ⁻¹)	NO ₃ ⁻ (mg L ⁻¹)	pH
C1	1.65	11.03	1.27	9.83	4.61	2.34	1.34	0.44	7.2
C2	1.75	8.62	1.05	7.10	4.695	2.41	2.48	1.28	n.m.
C3	1.35	5.83	1.26	5.34	2.96	2.85	1.64	0.34	7.4
C4	1.85	13.72	1.44	7.02	2.91	2.58	4.24	1.45	n.m.
C5	1.62	12.43	1.47	7.56	2.88	2.25	2.94	0.00	n.m.
C6	1.33	11.78	1.28	5.73	1.52	2.97	3.58	0.00	n.m.
C7	1.71	11.89	1.92	6.69	3.45	4.29	10.60	0.00	n.m.
C8	1.64	12.61	1.77	10.07	4.69	3.30	23.46	0.42	n.m.
C9	1.26	23.25	1.40	7.78	2.53	3.57	48.30	0.00	n.m.
C10	1.53	10.64	1.88	5.38	2.08	2.54	4.10	0.34	n.m.
C11	1.28	11.26	1.64	5.49	1.41	2.48	2.51	0.22	7.3
C12	1.31	10.98	1.29	5.76	1.13	4.01	4.62	1.35	n.m.
C13	1.17	12.31	1.49	4.34	1.21	2.37	3.32	0.37	7.6
C14	1.68	13.23	1.45	9.16	3.52	3.41	11.48	0.40	n.m.
C15	1.64	10.74	1.34	8.23	4.75	2.89	6.03	0.00	7.4
C16	1.30	9.13	1.30	5.18	3.07	2.22	3.18	0.19	n.m.
C17	0.92	9.17	1.07	5.65	2.48	1.91	2.83	0.45	7.4
C21	2.00	7.58	2.12	6.02	4.11	2.70	2.93	0.61	7.2
C22	1.96	10.27	1.69	7.65	6.35	2.96	5.64	0.15	n.m.
C23	1.43	11.29	1.78	5.30	4.07	2.72	10.53	0.26	7.6
C25	1.02	4.63	1.30	5.04	3.82	2.30	2.15	0.34	n.m.
C26	1.34	9.52	1.07	8.53	4.28	2.22	1.74	0.62	7.3
C27	1.40	9.05	1.33	10.01	4.86	1.94	4.12	0.44	n.m.
C30	1.39	8.51	1.01	6.36	1.94	2.05	1.91	1.14	n.m.
C31	1.52	9.42	0.90	8.05	2.90	1.96	1.53	0.32	7.4

Note: "n.m." denotes data not measured.

TABLE A5 Major ion concentrations and pH measurements of the meltwater samples from the two outcrops (CYB and CYC) at the Cyuie site

Sample ID	NH ₄ ⁺ (mg L ⁻¹)	Ca ²⁺ (mg L ⁻¹)	K ⁺ (mg L ⁻¹)	Mg ²⁺ (mg L ⁻¹)	Na ⁺	Cl ⁻ (mg L ⁻¹)	SO ₄ ²⁻ (mg L ⁻¹)	NO ₃ ⁻ (mg L ⁻¹)	pH
CYB-03-B	n.m.	6.92	1.30	4.14	1.74	1.01	3.79	0.01	n.m.
CYB-03-D	1.80	6.28	1.06	2.76	0.97	1.08	2.21	0.02	n.m.
CYB-04-B	1.87	n.m.	n.m.	n.m.	n.m.	n.m.	n.m.	n.m.	n.m.
CYB-05-B	n.m.	7.26	1.32	3.91	1.31	0.95	1.73	0.01	8.9
CYB-05-C	2.09	n.m.	n.m.	n.m.	n.m.	n.m.	n.m.	n.m.	8.8
CYB-06-A	n.m.	6.26	1.12	3.51	1.98	1.86	1.54	0.04	8.8
CYB-06-B	3.09	n.m.	n.m.	n.m.	n.m.	n.m.	n.m.	n.m.	8.7
CYC-01-A	n.m.	7.07	3.00	3.89	147	207	2.28	0.08	n.m.
CYC-01-B	1.86	n.m.	n.m.	n.m.	n.m.	n.m.	n.m.	n.m.	9.1
CYC-01-C	n.m.	7.19	2.39	2.81	82.8	121	2.25	0.05	9.1
CYC-02-B	4.16	n.m.	n.m.	n.m.	n.m.	n.m.	n.m.	n.m.	n.m.
CYC-03-A	2.01	n.m.	n.m.	n.m.	n.m.	n.m.	n.m.	n.m.	8.8
CYC-03-C	3.30	6.85	1.63	6.47	5.61	5.02	3.46	0.03	9.0

Note: "n.m." denotes data not measured.

**FIGURE A1** Pictures of the plant materials used for radiocarbon dating for (a) S02, (b) CYC-01, and (c) CYB-03 ice samples. Pictures are taken by Beta Analytic Inc. [Colour figure can be viewed at [wileyonlinelibrary.com](https://onlinelibrary.wiley.com/terms-and-conditions)]**TABLE A6** Major ion concentrations and pH measurements of the meltwater samples from the Syrdakh ice wedge

Sample ID	NH ₄ ⁺ (mg L ⁻¹)	Ca ²⁺ (mg L ⁻¹)	K ⁺ (mg L ⁻¹)	Mg ²⁺ (mg L ⁻¹)	Na ⁺ (mg L ⁻¹)	Cl ⁻ (mg L ⁻¹)	SO ₄ ²⁻ (mg L ⁻¹)	NO ₃ ⁻ (mg L ⁻¹)	pH
S01	1.06	8.93	0.87	4.43	0.52	1.06	0.62	1.22	7.8
S02	0.86	9.97	1.28	5.21	1.02	3.81	0.89	0.47	8.7
S03	1.69	11.05	1.78	6.34	1.67	1.47	1.24	0.08	8.8
S04	1.58	10.39	1.27	5.76	1.05	1.61	1.22	0.00	8.9
S05L	1.74	9.76	1.41	9.17	1.46	1.57	1.03	1.25	8.9
S05R	n.m.	n.m.	n.m.	n.m.	n.m.	n.m.	n.m.	n.m.	8.9
S06L	2.11	5.97	1.38	5.22	3.21	1.70	2.44	0.26	9.1
S06R	n.m.	n.m.	n.m.	n.m.	n.m.	n.m.	n.m.	n.m.	9.1
S08	n.m.	n.m.	n.m.	n.m.	n.m.	n.m.	n.m.	n.m.	8.8

Note: "n.m." denotes data not measured.